Endocrinology, 2025, **166**, bqaf124
https://doi.org/10.1210/endocr/bqaf124
Advance access publication 3 September 2025
Research Article

Role of Serotonin on Gene Expression and Physiology in Human Cytotrophoblasts and Placenta

Nolwenn S. Morris,[1,2] Seth Guller,[1] Zhonghua Tang,[1] Yuan-Wei Zhang,[3] Erin C. Siegman,[4] Kristin M. Milano,[1] Gary Rudnick,[5] and Harvey J. Kliman[1]

[1]Department of Obstetrics, Gynecology and Reproductive Sciences, Yale University School of Medicine, New Haven, CT 06520, USA
[2]Learning Planet Institute, University of Paris Cité, ED474, 75006 Paris, France
[3]School of Life Sciences, Guangzhou University, Guangzhou 510006, China
[4]Fordham College, Fordham University, Bronx, NY 10458, USA
[5]Department of Pharmacology, Yale University School of Medicine, New Haven, CT 06520, USA

Correspondence: Nolwenn Morris, PharmD, PhD, Department of Obstetrics, Gynecology and Reproductive Sciences, Yale University School of Medicine, 310 Cedar Street, FMB 225, New Haven, CT 06510, USA. Email: nolwennsue.morris@yale.edu; or Harvey J. Kliman, MD, PhD, Department of Obstetrics, Gynecology and Reproductive Sciences, Yale University School of Medicine, 310 Cedar Street, FMB 225, New Haven, CT 06510, USA. Email: harvey.kliman@yale.edu.

Abstract

Serotonin (5-hydroxytryptamine; 5-HT) is transported into the human placenta through the serotonin transporter (SERT/SLC6A4) on the surface of the syncytiotrophoblast. During this transit, a significant amount of 5-HT becomes concentrated in the cytotrophoblast nucleus. We used immunochemistry, inhibitors of SERT and transglutaminase 2, and RNA sequencing to elucidate the mechanism and consequences of this nuclear localization. Exogenous 5-HT recapitulated the uptake of 5-HT into the trophoblasts and its preferential concentration in cytotrophoblast nuclei we observed in the intact placenta. Cystamine eliminated the staining of the nuclei in placental explants by exogenous 5-HT, suggesting that serotonylation mediated this phenomenon. This was confirmed by Western blots and immunoprecipitation that identified histone 3, and specifically the 5th glutamine residue in histone 3, as a site of serotonylation. Inhibiting SERT with escitalopram or transglutaminase 2 with cystamine blocked cytotrophoblast differentiation in vitro and led to marked changes in RNA expression. Of the 38 524 mRNAs identified in these trophoblasts, cystamine changed the expression of 1986 and escitalopram significantly altered 374. Both treatments altered the expression of 155 mRNAs either positively or negatively. The downregulated genes were involved with cell proliferation, morphogenesis, motility, and growth, whereas genes that were upregulated controlled cell survival and protection pathways. These findings suggest that maternal 5-HT promotes placental, embryonic/fetal, and organismal development through histone serotonylation and consequent alterations in gene expression. They raise the possibility that alterations in 5-HT flux in the placenta affect placental and fetal growth, as well as organismal somatic, neurologic developmental, and pathological trajectories.

Key Words: placenta, trophoblast, serotonin, transporter, serotonylation, histones

Abbreviations: 5-HT, 5-hydroxytryptamine; CYS, cystamine; FBS, fetal bovine serum; hPL, human placental lactogen; ICC, immunocytochemistry; IHC, immunohistochemistry; IP, immunoprecipitation; IPA, Ingenuity Pathways Analysis; MAOA, monoamine oxidase A; NBF, neutral buffered formalin; SEM, standard error of the mean; SERT, serotonin transporter; TPH1, tryptophan hydroxylase 1; TPM, transcripts per million; UB, unbound; γ-tub, gamma tubulin.

The human placenta originates from the trophoblast layer of the day 5 embryonic blastocyst. Over the next few days, these cells differentiate into an inner layer of mononuclear stem cells —the cytotrophoblasts—and an outer multinucleated syncytiotrophoblast layer (1). Serotonin (5-hydroxytryptamine; 5-HT) plays a central role in these early processes, as well as in later steps in embryonic and fetal development (2-8). Often only considered to be a neurotransmitter, 5-HT likely has this pivotal function because it regulates numerous physiological processes, including proliferation and differentiation (9-13). We previously demonstrated that 5-HT is transported from the maternal intervillous space of the human placenta via the serotonin transporter (SERT/SLC6A4), through the syncytiotrophoblasts, into the cytotrophoblasts, and is ultimately discharged to the villous core where it is taken up by fetal capillaries (14). We noted during these studies that the cytotrophoblast nuclei were highly stained for 5-HT. An explanation for this phenomenon was subsequently suggested by the novel studies of Farrelly et al (15), who demonstrated the covalent modification of histone glutamines by 5-HT through transglutaminase 2 in a process known as serotonylation (16). Protein serotonylation, especially of histones, has been shown to mediate an array of cellular processes, including vesicular transport (16, 17), cell proliferation (9, 10), and differentiation (11-13). We therefore speculated that serotonylation of nuclear proteins could explain their persistent staining. This study sought to confirm this hypothesis through a study of primary cultures of human cytotrophoblasts.

Received: 13 April 2025. **Editorial Decision:** 25 July 2025. **Corrected and Typeset:** 3 September 2025

Materials and Methods

Specimens

Term placentas were collected anonymously from nonlaboring patients undergoing elective repeat cesarean sections who delivered healthy babies. The patients who supplied the placentas for the RNA sequencing studies delivered at 39 + 1, 39 + 2, and 39 + 3 weeks' gestation, and all other placentas were delivered between 39 and 40 weeks' gestation. All the women who provided term placental samples signed an informed consent (Yale institutional review board protocol 12696 through the Reproductive Sciences Biobank). Although individual demographics for these patients were not made available to the researchers, the general population demographics at Yale New Haven Hospital are as follows: non-Hispanic (82%), Hispanic (15%), unknown (3%), White (68%), Black (13%), Other (12%), Asian (6%), American Indian (0.7%), Pacific Islander (0.2%). For histologic and immunohistochemical evaluations, portions of each placenta were fixed in 10% neutral buffered formalin (NBF) for at least 1 day, embedded in paraffin, after which 5-µm sections were placed on coated glass slides designed for immunohistochemistry (IHC) processing.

Explant Culture

Samples for explant cultures were obtained as previously described (14). Briefly, fine placental slices of central parenchyma were repeatedly cut with a sterile surgical blade until pieces approximately $5 \times 3 \times 3$ mm were produced. These were placed in 6-well plates (CELLSTAR #657160 6-well cell culture plate, Greiner Bio-One North America, Monroe, NC) and incubated in F12 medium with 5-HT with or without inhibitor for 1 or 6 hours in humidified 5% CO_2-95% air at 37 °C; serotonin hydrochloride (H9523; CAS 153-98-0) and cystamine (Cys, C121509; CAS 56-17-7) were from Sigma-Aldrich, St. Louis, MO. 5-HT was used at 3 µM based on platelet activation studies (18); cystamine was used at 1 and 10 mM, as previously established (19). The explants were then washed with pH 7.4 PBS, fixed with NBF for 10 minutes, washed with PBS, and stored in 0.1% sodium azide in PBS at 4 °C until processed for IHC. The explants were then assessed for immunoreactivity in the outer (ie, most peripheral) 1 to 10 villus cross sections of each explant, as previously described (14). Three or more experiments were performed for each experimental condition.

Antibodies

The following rabbit polyclonal antibodies were used: anti-serotonin (Sigma-Aldrich, S5545, RRID:AB_477522, used at 0.016 µg IgG/mL for IHC and immunocytochemistry (ICC) and 1.6 µg IgG/mL for Western blotting); anti-monoamine oxidase A (MAOA; Santa Cruz Biotechnology, Dallas, TX, sc-20156, RRID:AB_2137260, used at 0.063 µg IgG/mL); anti-tryptophan hydroxylase 1 (TPH1; Sigma-Aldrich, HPA022483, RRID:AB_1858378, used at 0.5 µg IgG/mL); anti-SERT (LifeSpan BioSciences, Shirley, MA, LS-C179236, RRID: AB_3696655, used at 0.5 µg IgG/mL); anti-H3 (ThermoFisher, Waltham, MA, 855R2, RRID:AB_2792722, used at 0.2 µg IgG/mL), anti-H3Q5ser (Sigma-Aldrich, ABE1791, RRID:AB_3696656, used at 1 µg IgG/mL), anti-ferritin (Rockland Immunochemicals, Limerick, PA, 200-401-090, RRID:AB_2612112, used at 1 µg IgG/mL); anti-human placental lactogen (hPL; Agilent Technologies, Santa Clara, CA, A0137, RRID:AB_2631228, used at a 1:40 000 dilution, ~0.05 ng IgG/mL), anti-gamma-tubulin (γ-tub; Sigma-Aldrich, T5326, used at 1;2000, RRID:AB_532292, used at 1:2000); and, as a negative control, normal rabbit serum (Sigma-Aldrich, R9133, RRID:AB_3696658, used at 1 µg IgG/mL).

Immunohistochemistry

Five-micron serial sections were immunohistochemically stained using EnVision+ HRP Rabbit DAB+ (Agilent Technologies, K4011), as previously described (14, 20).

Trophoblast Purification

Cytotrophoblasts were prepared from fresh human term placentas by trypsin digestion and Percoll gradient fractionation, with the addition of an anti-CD9 and CD45 magnetic bead purification step, as previously described (21, 22). During the initial steps of the digestions and up to the magnetic purification step, 10% fetal bovine serum (FBS, Gemini Bio-Products, Broderick, CA, 100-106) diluted in DMEM/F12 (Gibco, ThermoFisher Scientific, 11330-032) with 4 mM L-glutamine, 1% penicillin/streptomycin was utilized. After the magnetic purification step, no FBS was added to the culture media, unless specifically noted. Cytotrophoblasts were then diluted to 1×10^6 cells per mL in DMEM/F12 with 4 mM L-glutamine, 1% penicillin/streptomycin, and either: (1) pelleted immediately by centrifugation for a zero-time point or (2) cultured in 2- or 4-chamber Nunc Lab-Tek II Chamber Slide System slides (ThermoFisher Scientific) (0.4×10^6 cells per chamber) or 6-well plates (CELLSTAR #657160 6-well cell culture plates) (3×10^6 cells per well) for 24 to 96 hours in humidified 5% CO_2-95% air at 37 °C with or without serotonin hydrochloride (3 or 100 µM), with or without cystamine (1 or 10 mM), or with or without escitalopram oxalate ("Lexapro"; Sigma-Aldrich PHR1733; CAS 219861-08-2; 200 µM), a competitive inhibitor ($K_i = 2.5$ nM) of SERT. Escitalopram was used at a range of concentrations based on previously published studies (14, 23, 24). Purified cytotrophoblasts from 10 preparations were used for additional studies as described next.

Immunocytochemistry (ICC)

Purified cytotrophoblasts were incubated for 24, 48, 72, or 96 hours, washed with PBS, fixed with NBF for 10 minutes, washed with PBS, stored at 4 °C in 0.1% sodium azide PBS until processed for ICC. After washing the azide buffer away with fresh PBS, the slides were brought to room temperature and stained with antibodies in the same fashion as described for IHC. The chambers were counterstained with hematoxylin. For quantification of immunoreactivity, each well was inspected microscopically using a raster pattern to ensure that the entire specimen was examined. The percent of cells stained in four samples was averaged and the mean of averages and standard error of the mean (SEM) calculated. Positive control sections from a deidentified normal human appendix were analyzed concurrently with each batch of slides to ensure uniform immunoreactivity between replicate experiments.

Following ICC, 3 representative low-power fields from each chamber for each of 3 experiments under all the test conditions at all indicated time points were photographed using a Nikon Eclipse 80i light microscope (Nikon Instruments, Melville, NY) using the 4× objective and a 2.5× projector

lens with attached Nikon D3× digital camera (Nikon, Minato City, Tokyo, Japan) controlled by Camera Control Pro 2 (Nikon) running on a Mac Pro (Apple, Cupertino, CA). The resultant Nikon Extended Format images were processed in Adobe Photoshop (Adobe, San Jose, CA) running on an iMac (Apple). Images were normalized to fill all 256 gray levels with the Levels command in each individual RGB channel and then white-balanced across all the RGB channels. The resultant images were then analyzed with ImageJ (Wayne Rasband, Research Services Branch, National Institute of Mental Health, Bethesda, MD). Total cell area was assessed using LAB settings with cutoffs of L:0-230; A:0-255; B:0-255. The cell area stained by diaminobenzidine by ICC was assessed using HSB settings with cutoffs of H:0-90; S:10-255; B:0-235. Experiments were performed in triplicate and the results were presented as mean percent area ± SEM. Fusion index was calculated as the ratio of the number of nuclei in syncytia to the total nuclei number of nuclei. The data were analyzed and plotted using Prism (GraphPad Software, Boston, MA) with statistical analysis (1-way ANOVA test, $n \geq 3$, $P < .05$).

Serotonin Transport

Influx of serotonin into dispersed trophoblast cells was measured as described previously (24). In brief, 100 µL of cytotrophoblasts diluted to 0.5 million cells/mL were cultured for 15 hours in 96-well plates as described previously—but in the absence of added FBS—then washed once with 100 µL of PBS/CM (PBS containing 0.1 mM $CaCl_2$ and 1 mM $MgCl_2$) and incubated in PBS/CM for the indicated times at 20 °C with or without modulators. The time course studies were performed as described, but at 24, 72, and 96 hours. Uptake assays were initiated by the addition of [^{3}H]serotonin (20 nM final concentration) and run for 10 minutes. The assays were terminated by 3 rapid washes with ice cold PBS. The cells were then solubilized in 30 µL of 0.1 M NaOH for 30 minutes, after which 120 µL of Opti-Fluor (PerkinElmer, Shelton, CT) was added. Accumulated [^{3}H]serotonin was determined by liquid scintillation spectrometry in a PerkinElmer MicroBeta plate counter. The escitalopram inhibition was measured by incubating the cells with 20 nM [^{3}H]5-HT and escitalopram at a range of concentrations (0-100 nM) for 10 minutes, as described previously. Nonlinear regression fits of [^{3}H]5-HT influx data were performed with Origin 2021 version 9.8.0.200 (Origin Lab, Northampton, MA). [^{3}H]5-HT influx was expressed as a percentage of that measured in the absence of escitalopram.

Nuclear Purification

Purified cytotrophoblasts were incubated with 5-HT, cystamine, and escitalopram as described previously, washed with ice cold PBS 3 times by centrifugation at 13 000*g* for 10 minutes to remove cell debris. The cells were then homogenized in 10 mM HEPES pH = 7.9, 10 mM KCl, 1.5 mM $MgCl_2$, 0.34 M sucrose, 10% glycerol, phenylmethylsulphonyl fluoride, and 0.1% of Triton X 100, as previously described (15). The homogenate was further incubated on ice with agitation for 30 minutes, then centrifuged at 1300*g* for 5 minutes at 4 °C. The pellet (nuclei) was set aside, while the supernatant was centrifuged at 20 000 g at 4 °C for 5 minutes, resuspended with the homogenization buffer, and centrifuged a final time at 1300*g* for 5 minutes at 4 °C to obtain the cytoplasmic fraction.

Immunoprecipitation

Following the protocol provided by ThermoFisher and using the solution from the kit (ThermoFisher, Classic Magnetic IP/Co-IP Kit, #88804), 500 µg of proteins from the nuclear and cytoplasmic fractions were separately added to 3 µg of antibodies, then incubated overnight at 4 °C. The next day, 20 µL of Pierce Protein A/G Magnetic Beads were washed 5 times, first with Lysis buffer, then deionized water, as instructed by the manufacturer. Once washed, the beads were incubated with the nuclear and cytoplasmic antibody complexes for 1 hour at room temperature. The protein-antibody complexes were placed onto a magnetic stand to separate the beads from the solution. The solution was kept for analysis ("unbound" or UB samples). After 2 washes with lysis buffer, and then 4 to 5 with deionized water, the beads were incubated with 100 µL of elution solution for 10 minutes at room temperature. Last, 10 µL of neutralization buffer was added. After 2 to 3 washes with deionized water, it was noted that the beads for some samples were not pulled to the magnets because of what was assumed to be the formation of protein-antibody-DNA complexes. We therefore incubated all the complexes with DNase I (MilliporeSigma, 10104159001) at a final concentration of 40 µg/mL for 10 minutes. The beads were put back on the magnetic stand, washed twice with deionized water, and then used for Western blots.

Protein Extraction

Proteins were extracted from adherent cells cultured under the specified experimental conditions described previously. For each condition, cells were first washed with cold PBS to remove residual media and debris, followed by the addition of 500 µL of radioimmunoprecipitation assay buffer (150 mM NaCl ThermoFisher Scientific #10010023, 1% Triton X ThermoFisher Scientific #A16046.AE, 0.5% sodium deoxycholate SigmaAldrich #S1827, 0.1% SDS AmericanBio #AB01920-00100, 50 mM TRIS AmericanBio #AB02000-01000), supplemented with EDTA-free Protease Inhibitor Cocktail (Roche, #11836170001) and phosphatase inhibitor (Roche, #4906845001). The cells were then thoroughly scraped using a cell scraper to ensure complete detachment and lysis. The lysates were then collected into microcentrifuge tubes and centrifuged at maximum speed for 10 minutes at 4 °C using an Eppendorf 5415R refrigerated centrifuge. The supernatant was then transferred into new microcentrifuge tubes and kept on ice until analyzed. Protein concentrations were determined using the DC Protein Assay kit (Bio-Rad, #5000112) following the manufacturer's instructions. Absorbance measurements were recorded using a Vmax microplate reader (Molecular Devices).

Western Blots

Proteins were obtained either from the resultant IP step, directly extracted from plated cells, or purified nuclei using radioimmunoprecipitation assay buffer at pH 8. Thirty micrograms of total proteins were added to denaturing buffer (900 µL of Lamaeli 2X [Bio-Rad #1610737]), with 100 µL of β-mercaptoethanol

(American Bioanalytical, #AB1340-00030) to facilitate the breaking of cysteine bonds. The solution was then brought to 95 °C for 1 minute to ensure denaturization of the peptides and loaded without storage onto PROTEAN TGX gels (Bio-Rad, 12% Mini-PROTEAN TGX Precast Protein Gels, 15-well, 15 µL #4561046) and run through the gel with a running buffer (1.92 M Glycine (Sigma #1002729747), 250 mM TRIS (AmericanBio #AB02000-01000), 1% SDS (AmericanBio #AB01920-00100)) at pH 8.3 using a current of 130 V for 40 minutes. The gel was transferred onto a precut membrane (ThermoFisher, nitrocellulose membranes, 0.45 µm, #88018) with transfer buffer (192 mM Glycine (Sigma #1002729747), 25 mM TRIS (AmericanBio #AB02000-01000), 20% ethanol [Decon #64-17-5]), using a current of 100 V for an hour. The membrane was then saturated with 5% milk solution buffer for an hour. The membrane was incubated with a primary antibody overnight at 4 °C, then washed with PBS solution (Bio Basic 10X PBS solution #PD8117) with 1:1000 Tween 20, then incubated with the appropriate species secondary antibody linked to a horseradish peroxidase for 2 hours. After additional PBS with 1:1000 Tween 20 washes, chemiluminescent solution (ThermoFisher #34577) was added to reveal the staining of the primary antibodies, using an infrared imager (LI-COR Odyssey). Staining intensity was quantified using Fiji (ImageJ2-version:2.9/1.53t) software. The data were analyzed and plotted using Prism (GraphPad Software, Boston, MA) with statistical analysis (one-way ANOVA test, $n \geq 3$, $P < .05$).

RNA Sequencing

RNA sequencing quality control

Total RNA quality was determined by estimating the A260/A280 and A260/A230 ratios by Nanodrop (Nanodrop, ND-1000, ThermoFisher Scientific). RNA integrity was determined by running an Agilent Bioanalyzer 2100 gel, which measures the ratio of the ribosomal peaks. RNA Integrity Number were ≥6 for the samples analyzed.

RNA sequencing library prep

Using the Kapa RNA HyperPrep Kit with RiboErase (KR1351, Roche Diagnostics, Indianapolis, IN), rRNA was depleted starting from a normalized input of total RNA by hybridization of rRNA to complementary DNA oligonucleotides, followed by treatment with RNase H and DNase to remove rRNA duplexed to DNA. Samples were then fragmented using heat and magnesium. First-strand synthesis was performed using random priming. Second-strand synthesis incorporated dUTPs into the second-strand cDNA. Adapters were then ligated, and the library was amplified. Strands marked with dUTPs were not amplified, allowing for strand-specific sequencing. Indexed libraries that meet appropriate cutoffs for both quantity and quality were quantified by quantitative RT-PCR using a commercially available kit (KAPA Library Quant Kit, Roche Diagnostics, 07960298001) and insert size distribution determined with an Agilent Bioanalyzer (Agilent TapeStation 4200). Samples with a yield of ≥0.5 ng/µL were used for sequencing.

Flow cell preparation and sequencing

Sample concentrations were normalized to 2.0 nM and loaded onto an Illumina NovaSeq (San Diego, CA) flow cell at a concentration that yields 35 million passing filter clusters per sample. Samples were sequenced using 100-bp paired-end sequencing on an Illumina NovaSeq according to Illumina protocols. The 10-bp unique dual index was read during additional sequencing reads that automatically follow the completion of read 1. Data generated during sequencing runs were simultaneously transferred to the Yale Center for Genomic Analysis (New Haven, CT) high-performance computing cluster. A positive control (prepared bacteriophage Phi X library) provided by Illumina was spiked into every lane at a concentration of 0.3% to monitor sequencing quality in real time.

Data analysis and storage

Signal intensities were converted to individual base calls during a run using the system's Real Time Analysis software. Base calls were transferred from the machine's dedicated personal computer to the Yale High Performance Computing cluster via a 1-gigabit network mount for downstream analysis. Primary analysis—sample demultiplexing and alignment to the human genome—was performed using Illumina's CASAVA 1.8.2 software suite. The data were returned to the user if the distribution of reads per sample in a lane had a sample error rate of less than 2%. Data were retained on the Yale Center for Genomic Analysis cluster for at least 6 months, after which it was transferred to a tape backup system. Access to our data set has been made available through the National Institutes of Health National Center for Biotechnology Information Gene Expression Omnibus, accession number GSE299974.

Following RNA sequencing, low-quality reads were trimmed, and adaptor contamination was removed using Trim Galore (v0.5.0; Babraham Bioinformatics, Cambridge, UK). Trimmed reads were mapped to the human reference genome (mm10) using HISAT2 (v2.1.0) (25). Gene expression levels were quantified using StringTie (v1.3.3b) (26) with gene models (v27) from the GENCODE project (27). Differentially expressed genes were identified using DESeq2 (Differential Expression analysis using the negative binomial distribution; R program v1.22.1) (28). Transcripts per million (TPM) were calculated as previously described (29), whereas adjusted P values were calculated with DESeq2 using the Benjamini and Hochberg method (30). MA plots were generated by plotting the log2FoldChange vs log2(mean of normalized counts).

Ingenuity Pathways Analysis (IPA)

IPA (QIAGEN Inc., https://www.qiagenbioinformatics.com/products/ingenuity-pathway-analysis) (31) was used at an expression threshold of log2fold change of ≥1 or ≤−1 and adjusted P value of ≤.05 to analyze the gene impact, involvement and consequences, for top canonical pathways, upstream regulators, top molecular and cellular functions, top system development and functions, and top diseases and disorders. Excel and Word (Microsoft, Redmond, WA) was used for graphical representation.

Results

Uptake of 5-HT and Expression of Serotonin Pathway-related Proteins in Cultured Human Cytotrophoblasts

Freshly prepared cytotrophoblasts that were pelleted, fixed and IHC stained for 5-HT showed very strong surface staining

in most of the cells (Fig. 1A, panel a, arrowheads), as well as scattered cells with light to moderate cytoplasmic staining. In contrast, the nuclear reactivity varied between obvious staining to light or no staining. No IHC staining was observed for either TPH1 (enzyme entry EC 1.14.16.4; the rate-limiting enzyme for 5-HT biosynthesis) (Fig. 1A, panel b) or monoamine oxidase A (MAOA; EC 1.4.3.4; inactivates 5-HT by oxidative deamination) (Fig. 1A, panel c). Staining for the 5-HT transporter (SERT; SLC6A4) revealed obvious surface staining (Fig. 1A, panel d, arrowheads), consistent with its functional membrane localization, as well as occasional light cytoplasmic staining. However, unlike the 5-HT staining—which also revealed surface and cytoplasmic staining—there was no nuclear reactivity (Fig. 1A, panel d).

The immunoreactivity of these same cytotrophoblasts varied when cultured for 24 to 96 hours, a range of time that allows these cells to aggregate, fuse, and syncytialize (21). Between 24 and 72 hours of culture, there was no apparent 5-HT reactivity (Fig. 1B, panels a-c). At 96 hours, a rare cell contained cytoplasmic 5-HT (Fig. 1B, panel d, black arrowheads). In contrast, when 100 µM exogenous 5-HT was added to these cultures, robust uptake was observed (Fig. 1B, panels e-h). Quantification of 4 independent trophoblast culture experiments revealed a modest downward trend of 5-HT uptake (Fig. 1C). Most of the 5-HT was taken up by unfused trophoblasts within aggregates (Fig. 1B, panels e, g, and h, black arrowheads). Many of these same cells also exhibited strongly stained nuclei (black arrows). The syncytia were very lightly and diffusely stained at 72 and 96 hours (Fig. 1B, panels g and h, black asterisks).

Concomitant with syncytialization, which occurs mostly during the last 2 days of incubation, these cultured trophoblasts acquired the differentiation marker MAOA (Fig. 1B, panels i-l). The increased concentration of MAOA first in single cells at 48 hours (arrowheads in Fig. 1B, panel j), then in the syncytia (see asterisks in Fig. 1B, panels j-l) may be the cause of the reduced accumulation of 5-HT by these cells, especially at 48 hours (Fig. 1B, panel f and Fig. 1C). Consistent with this hypothesis was the strong staining of 5-HT in the single cells within aggregates and syncytia (arrowheads in Fig. 1B, panels g and h) compared to multinucleated syncytia (asterisks in Fig. 1B, panels g and h); this is plotted in Fig. 1C.

TPH1 was not detectable in these cultured cells at any time point (Fig. 1B, panels m-p). This finding concurs with those for the intact human and mouse placentas (see Figs. 4 and 7 in Kliman et al (14)). SERT was present throughout the 4 days in culture (Fig. 1B, panels, q-t). SERT staining increased somewhat over time in individual cells (arrowheads), as well as in syncytia (*). It was sometimes seen on cell surfaces (for example, see the lowest arrowhead in panel s), but more often in cytoplasmic bodies we took to be vesicles (see inset, panel t, arrowheads). By day 4, most of the SERT was found in the cytoplasm of syncytia (* in Fig. 1B, panel t). The SERT in the syncytia could have been delivered from the cytotrophoblasts by their fusion. For example, in Fig. 1B, panel t and its inset, the stain was most intense in what may have been newly fused cells and became most dispersed in what may have been older syncytia. The inset also shows a rare finding: SERT staining what appears to be the nuclear membrane.

In both the freshly prepared cytotrophoblasts and 5-HT-treated cultured trophoblasts described previously, nuclear 5-HT reactivity was clearly apparent (Fig. 1A, panel a, and 1B, panels e, g, and h). To test the hypothesis that this nuclear 5-HT expression was due to serotonylation of nuclear proteins, we examined the effect of cystamine, a specific inhibitor that blocks transglutaminase 2-mediated serotonylation (32).

Serotonylation in the Human Placenta (Explants and Cultured Trophoblasts)

When placental explants were cultured with 3 µM 5-HT for 1 hour, obvious cytotrophoblast nuclear 5-HT immunoreactivity was observed (Fig. 2A, panel a, arrows). Cytotrophoblast cytoplasmic 5-HT reactivity was also noted (arrowhead). However, there was no obvious staining in the cytoplasm or nuclei of the syncytiotrophoblasts. In the presence of 10 mM cystamine for 1 hour, the staining intensity remained approximately the same, with both cytotrophoblast nuclear (Fig. 2A, panel b, arrows) and cytoplasmic (Fig. 2A, panel b, arrowheads) reactivity. When the incubation time with only 5-HT was increased to 6 hours, the intensity of both the cytoplasmic and nuclear 5-HT immunoreactivity was concomitantly increased (Fig. 2A, panel c). Notably, in the presence of 10 mM cystamine and 3 µM 5-HT for 6 hours, no cytotrophoblast nuclear staining was noted (Fig. 2A, panel d, arrows), whereas light cytoplasmic staining was still present (arrowheads). To confirm that cystamine was not simply killing or making the trophoblasts globally nonfunctional, serial sections of the same explant cultures that were incubated for 6 hours with 3 µM 5-HT and either no cystamine (Fig. 2A, panel e) or with 10 mM cystamine added (Fig. 2A, panel f) were immunohistochemically stained for hPL (Chorionic Somatomammotropin Hormone 1), a hormone produced in large quantities by syncytiotrophoblasts in term placentas (33). The presence of hPL under these conditions not only validated that these cells were alive, but that they were able to synthesize a complex protein hormone. Under both conditions, strong hPL was noted in the syncytiotrophoblast cytoplasm (arrowheads). As would be expected, no hPL staining was noted in the cytotrophoblasts (arrows).

To investigate what proteins were serotonylated in the presence of exogenous 5-HT, we performed Western blots on cytotrophoblasts cultured for 48 hours in the presence of 5-HT, cystamine (CYS), CYS + 5-HT, escitalopram, and escitalopram + 5-HT (Fig. 2B). The 42-kDa band suggestive of actin monomer (G-actin)—is a protein known to be serotonylated (34). 5-HT exposure (5HT lane) resulted in a slight increase over the control (CTRL lane) for both the 42- and 18-kDa bands (presumably H3 at a molecular weight of 17-8 kDa; bracket), whereas the cystamine treatment (CYS lane) reduced both. Addition of 5-HT (CYS + 5-HT lane) modestly rescued the 5-HT reactivity for at least the 42-kDa band. Addition of escitalopram (escitalopram lane) modestly decreased the staining intensity, whereas addition of 5-HT (escitalopram + 5-HT lane) had a negligible effect on the 42-kDa band.

From the previous work of Farrelly et al (15), we speculated that the nuclear staining we observed in both the cultured human cytotrophoblasts (Fig. 1B, panels e, g, and h) and explant cultures (Fig. 2A, panels a and c) might be the result of serotonylated histone H3. We therefore performed immunoprecipitation (IP) on nuclear fractions of purified cytotrophoblasts cultured for 48 hours—without FBS—using antibodies against histone H3 (H3), ferritin, 5-HT, and nonimmune IgG as a negative control. Ferritin was added as a negative control because it had been shown previously to be involved

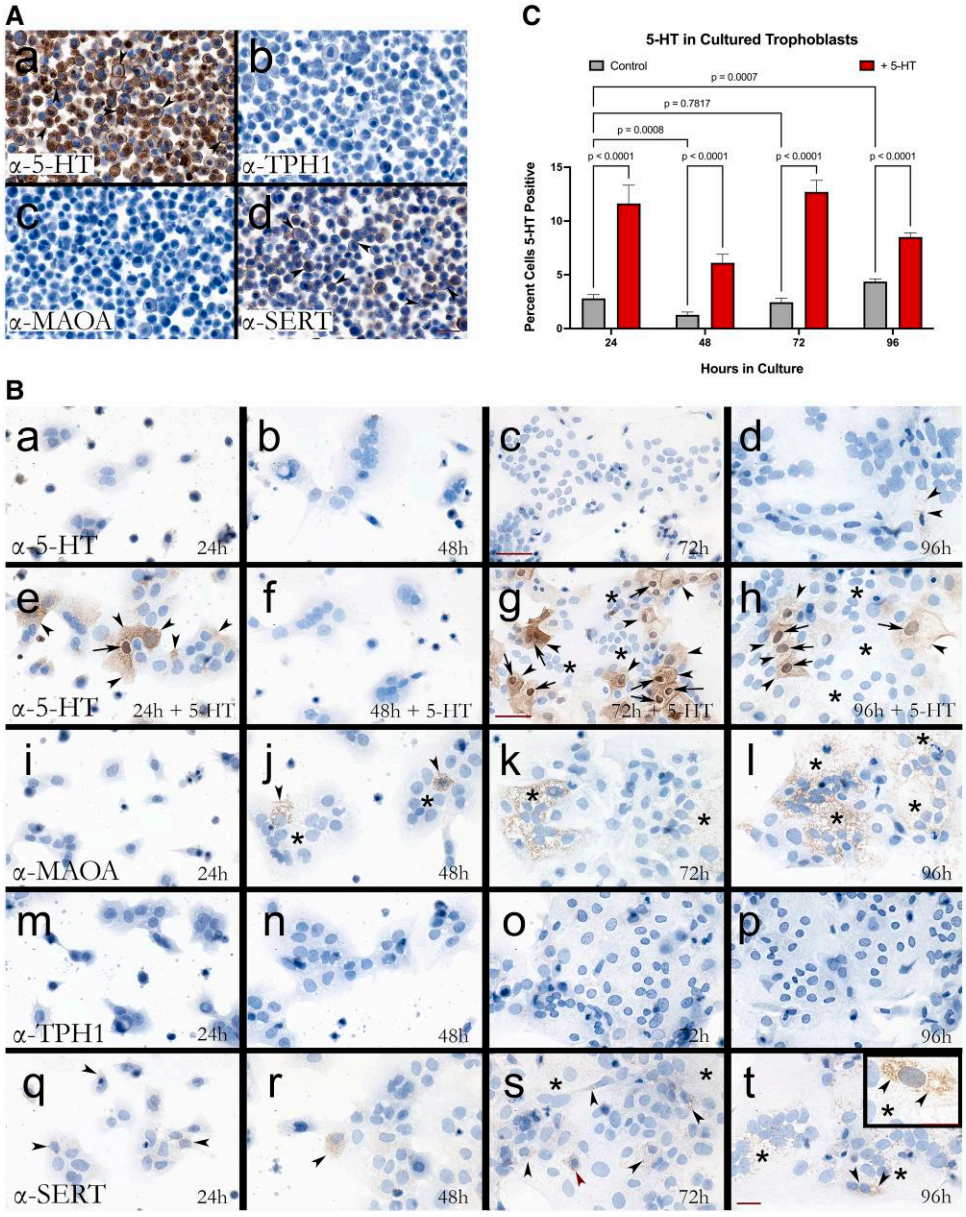

Figure 1. Serotonin and serotonin pathway proteins in purified and cultured cytotrophoblasts. (A) Immunoreactivity of freshly purified—"zero-time"—human cytotrophoblast cells. Cytotrophoblast cells were dispersed, purified, fixed as a pellet, and immunohistochemically stained. (a) 5-HT was present on the surface (arrowheads), in the cytoplasm, and in most nuclei. No TPH1 (b) or MAOA (c) was observed in these cells. (d) SERT was present on the surface of the majority of the cytotrophoblasts (arrowheads), with some cells also showing cytoplasmic staining. Scale bar = 25 μm. (B) Changes in the immunoreactivity of 5-HT, MAOA, TPH1, and SERT in trophoblast cells over time in culture. Purified trophoblast cells from human placentas were cultured for 24 to 96 hours in Nunc Lab-Tek II Chamber Slide System slides, 0.4×10^6 cells per chamber, then stained for 5-HT (a-d). Light 5-HT reactivity was only noted after 4 days of culture (arrowheads). (e-h) As in panels a-d, except that 100 μM exogenous 5-HT was present throughout. Staining occurred mostly in individual cells (arrowheads) scattered within aggregates. Staining was both cytoplasmic (arrowheads) and, more prominently, nuclear (arrows). Syncytia (*) were very lightly and diffusely stained at 72 and 96 hours. (i-l) As in panels a-d except that cells were stained for MAOA. Staining increased over 96 hours, appearing first in some individual cells within aggregates (arrowheads), followed by an increase in the staining of syncytia (*) between 48 and 96 hours. (m-p) As in panels a-d, except that cells were stained for TPH1. No reactivity was noted. (q-t) As in panels a-d, except that cells were stained for SERT. Immunoreactivity was observed at all time points, initially in a sparse punctate pattern (arrowheads) but, over time, increasingly diffusely in the syncytia (*). An occasional cell appeared to express surface staining (panel s, lowest arrowhead). Inset in panel t shows strong cytoplasmic SERT staining (arrowheads) in a recently fused cytotrophoblast within a syncytial cytoplasm (*). This same cell exhibited SERT nuclear membrane staining. Scale bar in panel t denotes 25 μm for all images except c and g. Scale bars in c and g denotes 25 μm. (C) Quantification of 5-HT immunoreactivity in trophoblasts represented in Fig. 1B, panels a-d compared to e-h. Addition of exogenous 5-HT resulted in a significant increase in intracellular and intranuclear 5-HT at all time points studied. Error bars are SEM from 4 independent experiments, with significance being defined as $P < .05$.

in cellular differentiation (35) and bound to DNA but not H3 (36). During the IP procedure, we noted that the magnetic beads remained suspended with all the antibodies except the negative control IgG (Fig. 2C, panels a and c). Suspecting this may have been due to protein-DNA complexes, we added DNase to the mixtures, which apparently dissolved the complexes and facilitated the attachment of the magnetic beads to the magnetic stand (Fig. 2C, panels b and d). Western blots

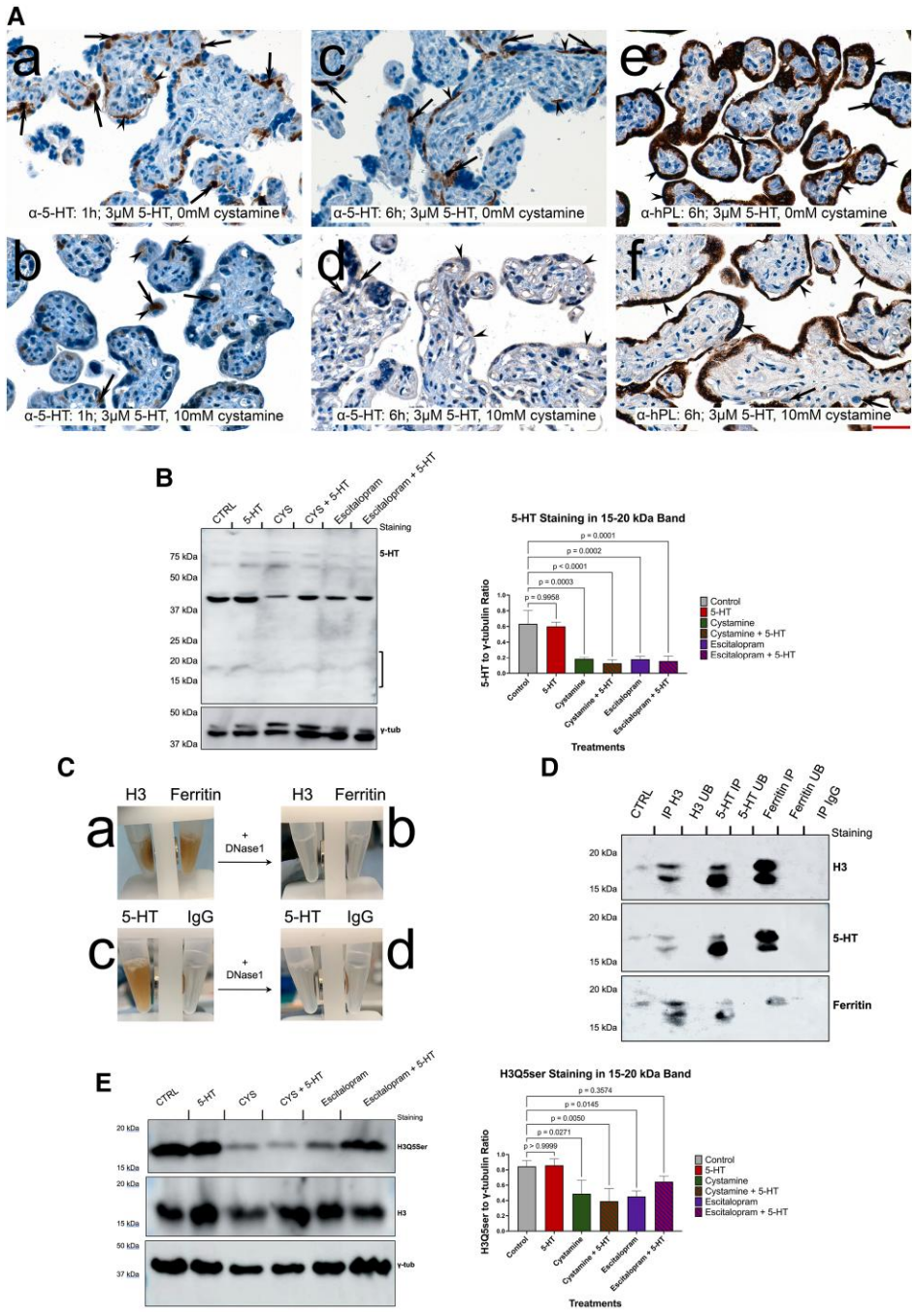

Figure 2. Evidence of serotonylation in trophoblasts. (A) Placenta explants treated with 5-HT with and without cystamine, an inhibitor of serotonylation (representative images from 1 of 3 experiments). (a) Explant treated with 5-HT for 1 hour revealed marked uptake of 5-HT into cytotrophoblast cytoplasm (arrowhead) and nuclei (arrows). (b) Addition of 10 mM cystamine resulted in decreased cytotrophoblast cytoplasmic staining (arrowheads), with persistent strong nuclear staining (arrows). (c) Increasing the incubation time of 5-HT alone to 6 hours resulted in even stronger cytotrophoblast cytoplasmic (arrowheads) and nuclear (arrows) reactivity. (d) Addition of 10 mM cystamine resulted in ablation of nuclear staining (arrows), whereas persistent light cytoplasmic reactivity was maintained (arrowheads). (e) Strong syncytiotrophoblast cytoplasmic hPL staining was present in control explants only treated with 5-HT (arrowheads), whereas the cytotrophoblast nuclei revealed no staining (arrows). (f) Addition of 10 mM cystamine did not change the hPL staining pattern. Panels a-f were at the same magnification; the scale bar in panel f denotes 50 μm. (B) Representative Western blot of cytotrophoblasts treated with 3 μM 5-HT, 10 mM cystamine (CYS), CYS + 5-HT, 200 μM escitalopram, and escitalopram + 5-HT stained with anti-5-HT antibodies. Gamma tubulin was utilized as a loading control (γ-tub), whereas untreated cytotrophoblasts serve as the control (CTRL) (n = 3). Quantification of the presumptive H3 band (bracket) to γ-tubulin ratio is shown to the right (treatments are noted along the x-axis and legend; *P* values represent comparisons of control to treatments), with significance being defined as $P < .05$. (C) Immunoprecipitation (IP) of cytotrophoblast nuclear proteins using antibodies against H3, ferritin, 5-HT, and the negative control IgG. (a) Anti-H3 and ferritin resulted in a suspension of beads that were not pulled out by the magnetic stand. (c) A similar suspension was seen with the anti-5-HT antibody. The IgG negative control beads bound tightly to the magnet. (b, d) Addition of DNase1 dispersed the suspension and facilitated the magnetic pull-down. (D) Western blots of IP fractions shown in panel C stained with antibodies against H3, 5-HT, and ferritin (n = 3). (E) Representative Western blot of purified cytotrophoblast nuclei treated with 3 μM 5-HT, 10 mM cystamine (CYS), CYS + 5-HT, 200 μM escitalopram, and escitalopram + 5-HT stained with antibodies specific for H3 serotonylated on the 5th glutamine (H3Q5Ser), H3, and gamma-tubulin as a loading control (γ-tub), whereas untreated cytotrophoblasts serve as the control (CTRL) (n = 3). Quantification of the H3Q5ser band to γ-tubulin ratio is shown to the right (treatments are noted along the x-axis and legend; *P* values represent comparisons of control to treatments), with significance being defined as $P < .05$.

of both the IP and unbound (UB) fractions revealed a complex pattern of associations (Fig. 2D). First H3 IP stained with anti-H3 antibody (Fig. 2D, IP H3 lane, top row) at molecular weights of ~17 and ~18 kDa, consistent with H3 being present in this precipitate. There was no reactivity against the H3 UB fraction (lane 3, top row). There was very strong staining of the 5-HT IP fraction by anti-H3 (Fig. 2D, 5-HT IP lane, top row) at the same molecular weights, but again none in the 5-HT UB fraction. Even stronger H3 staining was noted in the ferritin IP fraction (Fig. 2D, ferritin IP lane, top row), but again, not in the UB fraction. No staining was noted with the IgG IP fraction (last lane). When anti-5-HT was used as the primary antibody in the Western blot, similar results were seen (Fig. 2D, middle row). When anti-ferritin antibody was utilized (Fig. 2D, lower row), the results were similar to the top and middle rows, except that the ~18-kDa band in the 5-HT IP fraction revealed minimal reactivity, whereas the ~17-kDa band in the ferritin IP fraction showed no staining (Fig. 2D, ferritin IP lane, lower row). The control lane (CTRL), which represented the starting homogenate without IP, revealed faint bands at ~18 kDa that were reactive with all 3 antibodies used for Western blot staining.

The availability of an antibody reactive against the serotonylated glutamine 5 on histone H3 (H3Q5ser) (15) allowed us to further explore the regulation of this posttranslational mark in cultured human cytotrophoblasts. Western blots of untreated cytotrophoblasts cultured for 48 hours revealed strong bands at ~18 kDa when stained with the anti-H3Q5ser and anti-H3 antibodies (Fig. 2E, CTRL lane). Addition of 5-HT to the cultures did not alter either band, suggesting that sites for this serotonylated mark were already saturated under our control culture conditions. When treated with cystamine, the H3Q5ser band decreased, whereas the H3 band remained relatively unchanged (Fig. 2E, CYS lane). Addition of 5-HT to the cystamine treatment did not rescue this inhibition (Fig. 2E, CYS + 5-HT lane). Addition of the SERT inhibitor escitalopram also decreased the degree of serotonylation (Fig. 2E, escitalopram lane), which was modestly counteracted when exogenous 5-HT was added (Fig. 2E, escitalopram + 5-HT lane).

RNA Expression in Cultured Human Cytotrophoblasts

To better understand the impact of both cystamine and escitalopram in our system, we performed RNA sequencing on cultured cytotrophoblasts derived from 3 separate term placentas under a variety of treatment protocols. A heat-map of our results is shown in Fig. 3A. The gestalt overview was that cystamine induced a significant alteration of RNA expression, while escitalopram induced a more modest modulation of trophoblast RNA expression. Global quantification of the 38 524 RNAs analyzed revealed that 36 164 (93.87%) remained unchanged, while cystamine altered 1986 (5.16%), and escitalopram modified 374 (0.97%) (Fig. 3A, pie chart). The addition of exogenous 5-HT to each of the treatment groups had minimal effect on the overall RNA expressions (see hatched columns, Fig. 3A). TPM expressions of a select group of 26 genes are shown in Fig. 3B. Significant (based on mean adjusted P values from 3 separate placentas) alterations in RNA expressions are demarcated by asterisks (P adjusted values ranged from 0.041 to 6×10^{-7}). Some genes were expressed at very high levels and were not significatively altered with either treatment (for example glycoprotein α and ferritin light chain); others showed significant increases with cystamine treatment (for example, mitochondrial cytochrome C oxidase 1, heat shock 90α A1, and ubiquitin B), whereas other genes showed significant suppression with both cystamine and escitalopram treatments (for example, pregnancy-specific ß1-glycoprotein 5, syndecan 1, and human chorionic gonadotrophin ß5). The graph also makes it clear that the number of RNAs produced per gene varied markedly in these cultured trophoblasts, with control levels of glycoprotein α at a high of 36 489 TPM, whereas both tryptophan hydroxylases (TPH1 and TPH2) were each expressed at the lowest levels at 0.019 TPM.

Impact of Escitalopram on Human Cultured Trophoblasts

Since escitalopram altered the mRNA expression of cultured trophoblasts, we wanted to next see what impact this SERT inhibitor had on the morphologic differentiation of cultured cytotrophoblasts. In a word, escitalopram had a marked impact on these cells, starting at the earliest time point examined (Fig. 4A). The control cells treated with 100 µM 5-HT for 24 hours flattened on the culture surface and began to aggregate (Fig. 4A, panel a), a process of morphologic differentiation that freshly purified, healthy cytotrophoblasts undergo in culture (21). Most of the cells were immunohistochemically reactive when stained with anti-5-HT antibody (Fig. 4A, panel a inset, arrows), while scattered cells remained negative (arrowheads). In marked contrast, the addition of 200 µM escitalopram resulted in virtually no flattened cells (implying no morphologic differentiation), the majority of which were 5-HT negative (Fig. 4A, panel b, inset, arrowheads). An occasional cell contained 5-HT (arrow). The control cells at 48 hours were like the 24 hours cells, except that more syncytia were noted (Fig. 4A, panel c, inset). Both 5-HT positive (arrows) and negative (arrowheads) were easily identified. Again, the 48 hours escitalopram treated cells remained as small rounded 5-HT negative individual cells (Fig. 4A, panel d, inset, arrowheads), suggesting the absence of morphologic differentiation under this condition. Interestingly, a few 5-HT positive flattened cells could be seen. Upon close examination, these appeared to be migrating macrophages, identified by their bean-shaped nuclei and expansive cytoplasmic extensions (Fig. 4A, panel d, inset, arrow). After 72 hours in culture, the control trophoblasts had largely syncytialized, the majority of which were 5-HT negative (Fig. 4A, panel e, inset arrowheads). As was seen in Fig. 1B, panels g and h, the only cells that were 5-HT positive were the unfused cells within the aggregates (Fig. 4A, panel e, inset, arrows). In contrast, there were very few cells seen with escitalopram treatment, and the few adherent cells were round and 5-HT negative (Fig. 4A, panel f, inset, arrowheads). Again, the few 5-HT-positive cells appeared to be migrating macrophages (inset, arrow). To confirm that the escitalopram treatment was not simply resulting in rounded dead cells, we incubated cytotrophoblasts for 48 hours with only 3 µm 5-HT with and without escitalopram and stained the cultures with anti-hPL antibodies. Reducing the 5-HT levels to 3 µM in the presence of the same 200 µM of escitalopram ensured there was a molar excess of this SERT inhibitor. Only scattered trophoblasts were hPL positive in the none-treated cultures (Fig. 4A, panel g, inset, arrow). Interestingly, the few macrophages noted were hPL

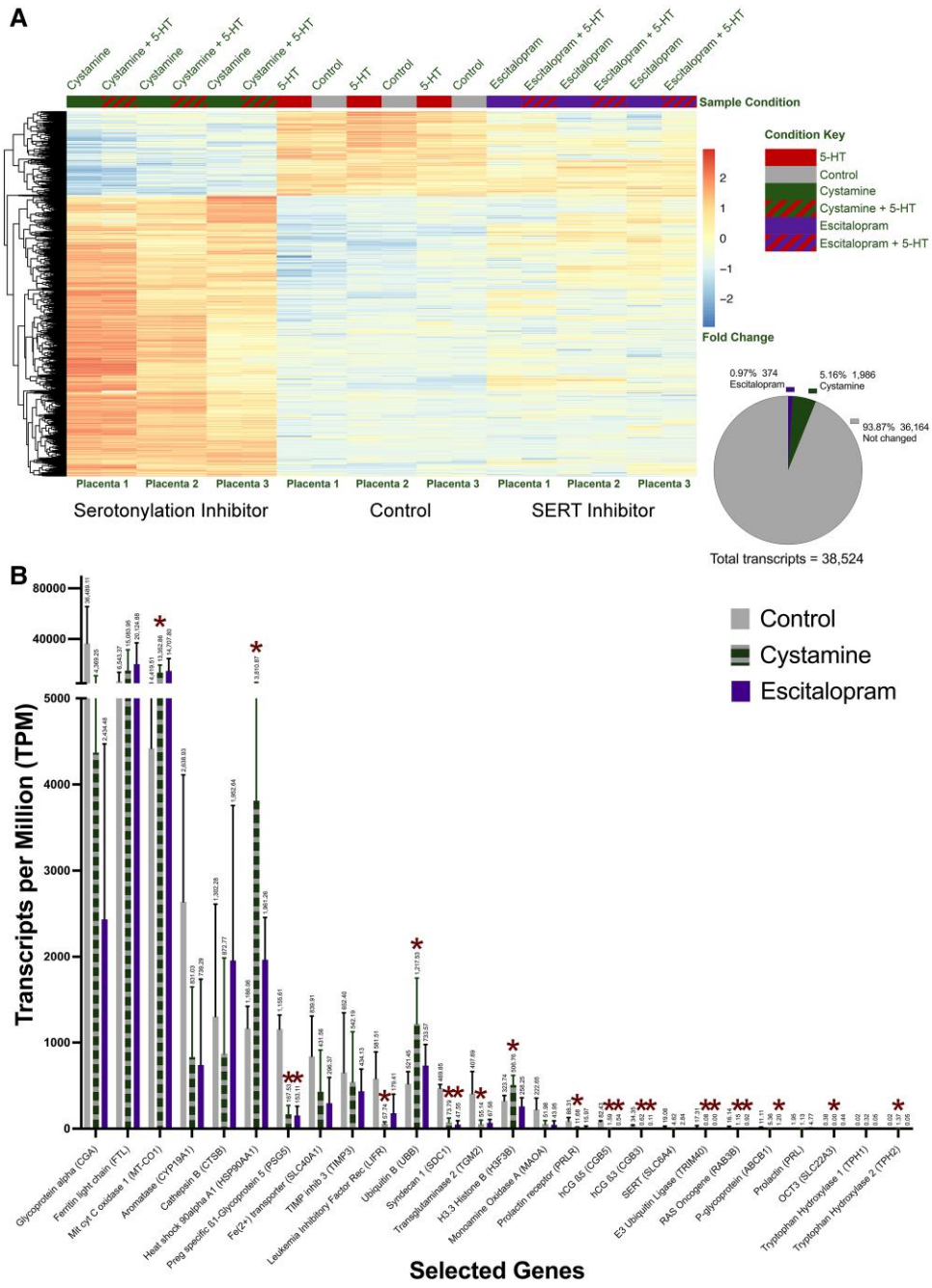

Figure 3. Up- and downregulation of cytotrophoblast genes. (A) Heat map of mRNA expression in cytotrophoblasts purified from 3 different placentas treated with 3 μM 5-HT, 10 mM cystamine, and 200 μM escitalopram, as indicated. The pie-chart documents the total number of mRNAs produced (gray), those altered by cystamine (green), and escitalopram treatments (purple). (B) Transcripts per million (TPM) mRNAs produced under control, cystamine, and escitalopram treatments of selected genes. Asterisks indicate significant differences in the mean adjusted *P* values (30) from 3 different placentas (*P* adjusted values ranged from 0.041 to 6×10^{-7}).

negative (arrowhead), as would be expected because these cells do not synthesize hPL. When exposed to escitalopram, the expected marked decrease in cell number was observed as well as the lack of cell flattening (Fig. 4A, panel h); however, even in the presence of this many-fold molar excess of escitalopram, the rounded cells were hPL positive (inset, arrows), suggesting these cells were still biologically active and able to synthesize a complex protein hormone usually only seen in well-formed syncytiotrophoblasts (21).

To confirm that escitalopram was acting on these cultured trophoblasts via the SERT transporter, we performed influx studies with radioactive 5-HT (Fig. 4B). 5-HT influx into these cells was NaCl dependent, as would be expected for SERT (37). Similarly, the 5-HT influx was significantly inhibited with 3 known SERT antagonists (fluoxetine, paroxetine, and imipramine). A substrate-velocity curve in the presence of varying concentrations of escitalopram revealed a Ki of 0.54 ± 0.14 nM, which confirmed that the serotonin transporter in these cultured trophoblasts is biologically the same as is seen in other cell types, including the prototypical SERT-containing cell, the human platelet (37). Interestingly, when the influx experiments were performed with

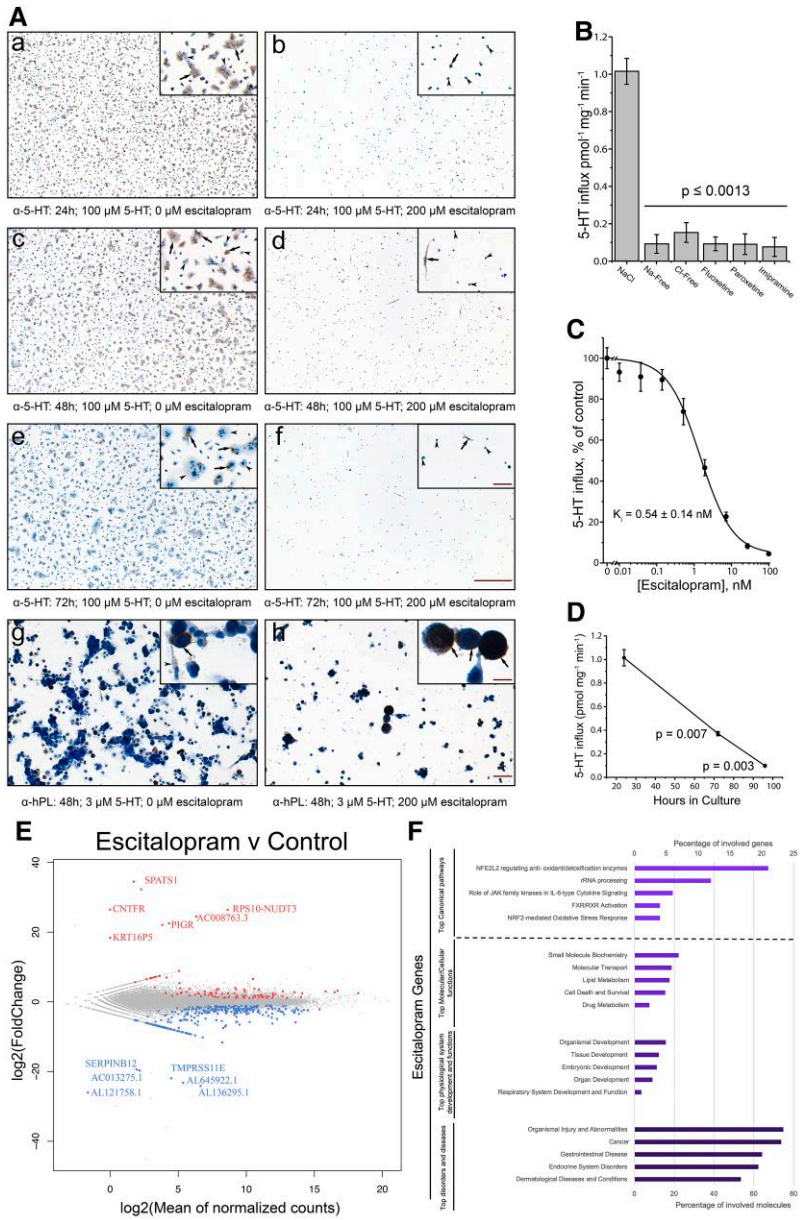

Figure 4. Effects of escitalopram on in vitro growth, 5-HT influx, and gene expression of purified trophoblasts. (A) Impact of escitalopram on cultured trophoblasts. (a) Trophoblasts cultured in Nunc Lab-Tek II Chamber Slide System slides, 0.4×10^6 cells per chamber exposed to 100 μM 5-HT for 24 hours flattened, aggregated, and began to syncytialize (morphologic differentiation (21)). Many cells avidly took up the amine (inset, arrows), whereas some cells did not (inset, arrowheads). (b) Addition of 200 μM escitalopram blocked virtually all cells from morphologically differentiating. An occasional cell contained 5-HT (inset, arrow), whereas most remained rounded with no immunoreactive 5-HT (inset, arrowheads). (c) Culturing for 48 hours revealed more and larger aggregates and syncytia. Again, many (but not all; inset, arrowheads) of these cells contained 5-HT (inset, arrows). (d) Escitalopram exposure for 48 hours again prevented morphologic differentiation, with no trophoblasts noted to contain 5-HT (inset, arrowheads). The few flattened, 5-HT-positive cells were macrophages, as identified by their bean-shaped nuclei (inset, arrow). (e) After 72 hours of culture, virtually all the trophoblasts had syncytialized, but were now 5-HT negative (inset, arrowheads). The 5-HT-positive trophoblasts were single trophoblasts that had recently fused with a negative syncytium (inset, arrows). (f) Exposure to 72 hours of escitalopram resulted in a marked reduction in total cell numbers, of which the trophoblasts were virtually all 5-HT-negative rounded cells (inset, arrowheads). The few 5-HT-positive cells present were motile macrophages (inset, arrow). To ensure that these treatments were not simply lethal, trophoblasts were incubated without (g) and with (h) escitalopram for 48 in the presence of 3 μM 5-HT and stained with hPL, a marker of trophoblast viability and biosynthetic activity. Positive hPL trophoblasts were seen under both conditions (insets, arrows). Macrophages were also noted in these cultures, but they were, as expected, hPL negative (g, inset, arrowhead). The scale bar in panel f denotes 500 μm for panels a-f. The scale bar in inset f denotes 83 μm for all a-f insets. The scale bar in panel h denotes 63 μm for panels g and h. The scale bar in inset h denotes 21 μm for g and h insets. (B) In the presence of NaCl, 5-HT was actively taken up by 15-hour purified trophoblasts. Removal of either Na or Cl led to a marked decrease in transport, confirming the NaCl dependent SERT mechanism in these cells. Further validation of this transport being SERT dependent was confirmed by inhibiting influx with the addition 1 μM of known the SERT competitive inhibitors fluoxetine, paroxetine, and imipramine. (C) Representative kinetic analysis of 5-HT flux with triplicate measurements. The Ki value for escitalopram inhibition was estimated to be 0.54 ± 0.14 nM, which represents the mean ± SEM from 3 experiments. (D) A time course of 5-HT influx from 24 to 96 hours revealed a linear decrease in transport over the times studied (n = 3 and significance was confirmed at $P < .05$). (E) MA plot of mRNAs (created by plotting the log2 Fold Change (y-axis) vs log2(Mean of normalized counts) (x-axis) of all genes as reported by DESeq2) that were either significantly upregulated (upper data points) or downregulated (lower data points) with escitalopram treatment. The 12 highest fold changed coding genes are labelled. (F) IPA analysis of these genes revealed the key pathways, functions, and diseases associated with all the escitalopram-altered genes.

trophoblasts that were cultured for 24-96 hours prior to the study, the rate of uptake dropped in a linear fashion over this time (Fig. 4D).

Once we assessed cultured trophoblast morphologic differentiation and 5-HT transport, we analyzed the genes most impacted by escitalopram. Of the 374 genes whose expression was altered with this treatment, 12 protein-coding genes had a greater than ±10 log2 expression fold change (Fig. 4E). IPA (Fig. 4F) revealed the most frequent top canonical pathway and molecular functions genes were related to antioxidant enzymes and pathways, rRNA processing, and Jak signaling, whereas the top physiological system genes were related to embryonic, tissue, organ, and organismal development; and the top disorders genes were related to injury and cancer.

Impact of Cystamine on Human Cultured Trophoblasts

To investigate the impact of serotonylation on cultured human cytotrophoblasts, we treated these cells with cystamine, an organic disulfide that inhibits tissue transglutaminase 2 serotonylation (38-40). As shown in Fig. 5A, when cytotrophoblasts were cultured for 24 hours in control media (Fig. 5A, panel a), they flattened out, aggregated, and started to syncytialize, a process known as morphologic differentiation (21) (inset, arrows). Occasional trophoblasts remained as flattened single cells (inset, arrowheads). In the presence of 1 mM cystamine (Fig. 5A, panel b), there were fewer cells overall and when examined, the majority were single cells (inset, arrowheads), with only occasional fused aggregates or syncytia (inset, arrow). Increasing the cystamine concentration to 10 mM resulted in a complete absence of aggregates or syncytia (Fig. 5A, panel c), with the few cells present being rounded trophoblasts (inset). Quantification of the degree of trophoblast fusion is shown in Fig. 5B. At 48 hours of culture (Fig. 5A, panel d), the control cells were mostly either in aggregates or syncytia (inset, arrows), with only scattered single flattened cells (inset, arrowhead). In the presence of 1 mM cystamine (Fig. 5A, panel e), there were again fewer cells overall and, when examined, the majority were single cells (inset), with only occasional fused aggregates or syncytia (inset, arrow). Of note, one of these single partially flattened cells was 5-HT positive (Fig. 5A, panel e, inset, arrowhead). At 10 mM cystamine, no aggregates or fused cells were noted (Fig. 5A, panel f). Intriguingly, the few remaining cells were often 5-HT positive (inset, arrowheads). At 72 hours, the control trophoblasts had mostly fused to become syncytiotrophoblasts (Fig. 5A, panel g, inset, arrow), with scattered flattened single cells (inset, arrowheads). Addition of 1 mM cystamine again resulted in fewer aggregates or syncytia, with scattered, unflattened single cells (Fig. 5A, panel h). The few syncytia present were 5-HT positive (inset, arrow) or contained a recently fused positive single cell (inset, arrowhead). Increasing the cystamine concentration to 10 mM for a full 72 hours led to the most severe effect (Fig. 5A, panel i), with no aggregates or syncytia noted and only a few scattered single rounded cells, some of which were 5-HT positive (inset, arrowhead). Trophoblasts grown for 48 hours in the presence of 0, 1, and 10 mM cystamine stained for hPL revealed similar morphologic patterns (Fig. 5A, panels j, k, and l), with flattened syncytia noted only in the 0-mM treatment group (arrow), but with hPL-positive, single rounded cells noted in all treatment conditions (arrowheads).

After assessing the phenotypic impact of cystamine, we analyzed the genes most impacted by this inhibitor. An MA plot (Fig. 5C) revealed that of the 1986 genes whose expression was altered by cystamine, 9 protein-coding genes had a greater than 10 log2 fold increase, whereas 5 protein-coding genes had a greater than 10 log2 fold decrease in expression. IPA analysis (Fig. 5D) revealed the most frequent top canonical pathway genes were related to rRNA processing, cell checkpoints, antioxidant, and detoxification enzymes; the top cellular and developmental genes were related to cellular development, proliferation, and tissue and organismal development; and the top disorder genes were related to injury, cancer, and gastrointestinal, reproductive, and hepatic system diseases.

Genes Common to Escitalopram and Cystamine Treatments

Since both escitalopram and cystamine appeared to impact cultured cytotrophoblasts in a morphologically similar way (compare Figs. 4A and 5A), we explored genes that were similarly altered by both treatments. Of the 1986 genes altered with cystamine treatment and 374 altered by escitalopram, 156 were altered by both (Fig. 6A). All these genes were concomitantly up- or downregulated, except for arrestin β 1, which showed a -0.49 log2 fold change with cystamine treatment and a +0.71 log2 fold change with escitalopram treatment. Removing this gene left 155 genes, 68 of which were upregulated and 87 were downregulated by both treatments (Fig. 6B). The individual 68 upregulated genes are shown in Fig. 6C, whereas the 87 downregulated genes are shown in Fig. 6D. The darker the shading of each cell, the larger the log2 fold change. IPA analysis (Fig. 6E) revealed many of the genes that were upregulated (red bars (top five of each set)) were active in detoxification, rRNA processing, cell death and survival, and molecule metabolism for molecular and cellular functions; the system and disorders genes were related to tissue morphology, brain development and behavior, injury, and skeletal disorders, to name a few. In contrast, the downregulated genes (blue bars (bottom five of each set)) were more often associated with hormone biosynthesis, signaling for molecular functions; the cellular and disorders of those genes were related to development and maintenance, cell-to-cell interactions, organ and organismal development; and finally, injury and cancer were the most frequent associated disorders.

When we focused on the genes involved with development, cell-to-cell interactions, growth, detoxification, and protection, we produced a representative list of 40 key genes that appeared to most likely be driving the responses seen with the escitalopram and cystamine treatments, and by extension, serotonylation in the trophoblasts we studied (Fig. 7).

Although not validated by quantitative PCR, many of the genes that were upregulated were involved in cell survival and protection pathways. Some intriguing examples included the following. Ciliary neurotrophic factor receptor (+30.7 log2 fold change) is involved with neuronal cell survival, differentiation, and gene expression. MATR3 (matrin 3; +8.6 log2 fold change) stabilizes mRNAs. HSPA6 (heat shock protein family A member 6; +8.4 log2 fold change) is a molecular chaperone that protects the proteome from a wide variety of stresses. Zinc finger protein 365 (+6.7 log2 fold change) maintains genomic stability. GSR (glutathione-disulfide reductase;

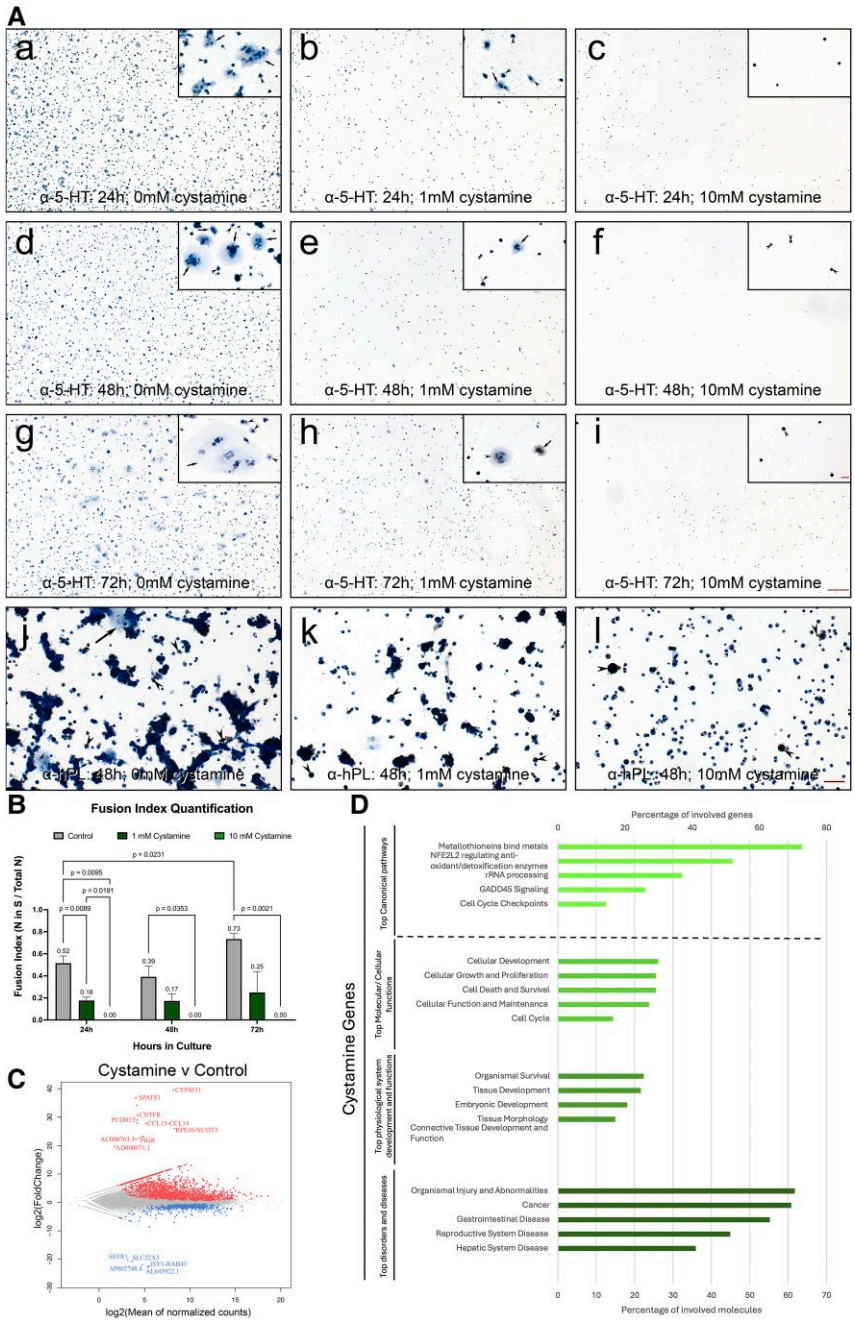

Figure 5. Effects of cystamine on in vitro growth, 5-HT influx, and gene expression of purified trophoblasts. (A) Impact of cystamine on cultured trophoblasts (panels a-i stained with anti-5-HT antibodies; panels j-l stained with anti-hPL antibodies). (a) Trophoblasts cultured in Nunc Lab-Tek II Chamber Slide System slides, 0.4×10^6 cells per chamber in the absence of cystamine for 24 hours revealed that single cytotrophoblasts had flattened (inset, arrowheads), aggregated, and even began to syncytialize (inset, arrows), in a process known as morphologic differentiation (21) (see also Fig. 4A). (b) In the presence of 1 mM cystamine, there were fewer flattened cells, most of which were individual cells (inset, arrowheads), with an occasional aggregate (inset, arrow). (c) The 10-mM cystamine treatment resulted in only scattered single, rounded cells. (d) Forty-eight hours of culture without cystamine yielded scattered, flattened single cells (inset, arrowheads), but most cells had aggregated and syncytialized (inset, arrows). (e) 1 mM cystamine treatment for 48 hours resulted in many rounded cells, an occasional syncytium (inset, arrow), and an occasional 5-HT-positive flattened trophoblast (inset, arrowhead). (f) 10 mM cystamine treatment led to very few rounded trophoblasts, many of which were 5-HT positive (inset, arrowheads). (g) 72 hour control cultures resulted in many large syncytia (inset, arrow) and scattered flattened single cells (inset, arrowheads). (h) After 72 hours in the presence of 1 mM cystamine only a few single rounded cells were noted, with occasional syncytia, which were sometimes 5-HT positive (inset, arrow). A recently absorbed, 5-HT positive, single trophoblast can be seen in one of the syncytia (inset, arrowhead). (i) Seventy-two hours of cystamine treatment resulted in only rare, rounded trophoblasts, some of which were 5-HT positive (inset, arrowhead). (j-l) When the trophoblasts were cultured for 48 hours with no (j), 1 mM (k), and 10 mM (l) cystamine similar morphologic patterns were observed, with syncytia noted (arrow) and single trophoblasts that were hPL positive (arrowheads), validating their viability and persistent biosynthetic ability. The scale bar in panel i denotes 630 μm for panels a-i, the scale bar in the inset in i denotes 63 μm for all insets, while the scale bar in panel l denotes 158 μm for panels j-l. (B) Quantification of trophoblast fusion and morphologic differentiation. Fusion index was calculated counting nuclei in syncytia divided by the total number of nuclei in three different placentas with or without cystamine at the time points noted (n = 3 and significance was defined as $P < .05$). (C) MA plot of mRNAs (created by plotting the log2FoldChange (y-axis) vs log2(Mean of normalized counts) (x-axis) of all genes as reported by DESeq2) that were either significantly upregulated (upper data points) or downregulated (lower data points) with cystamine treatment. The 14 highest fold-changed coding genes are labelled. (D) IPA analysis of these genes revealed the key pathways, functions, and diseases associated with all the cystamine altered genes.

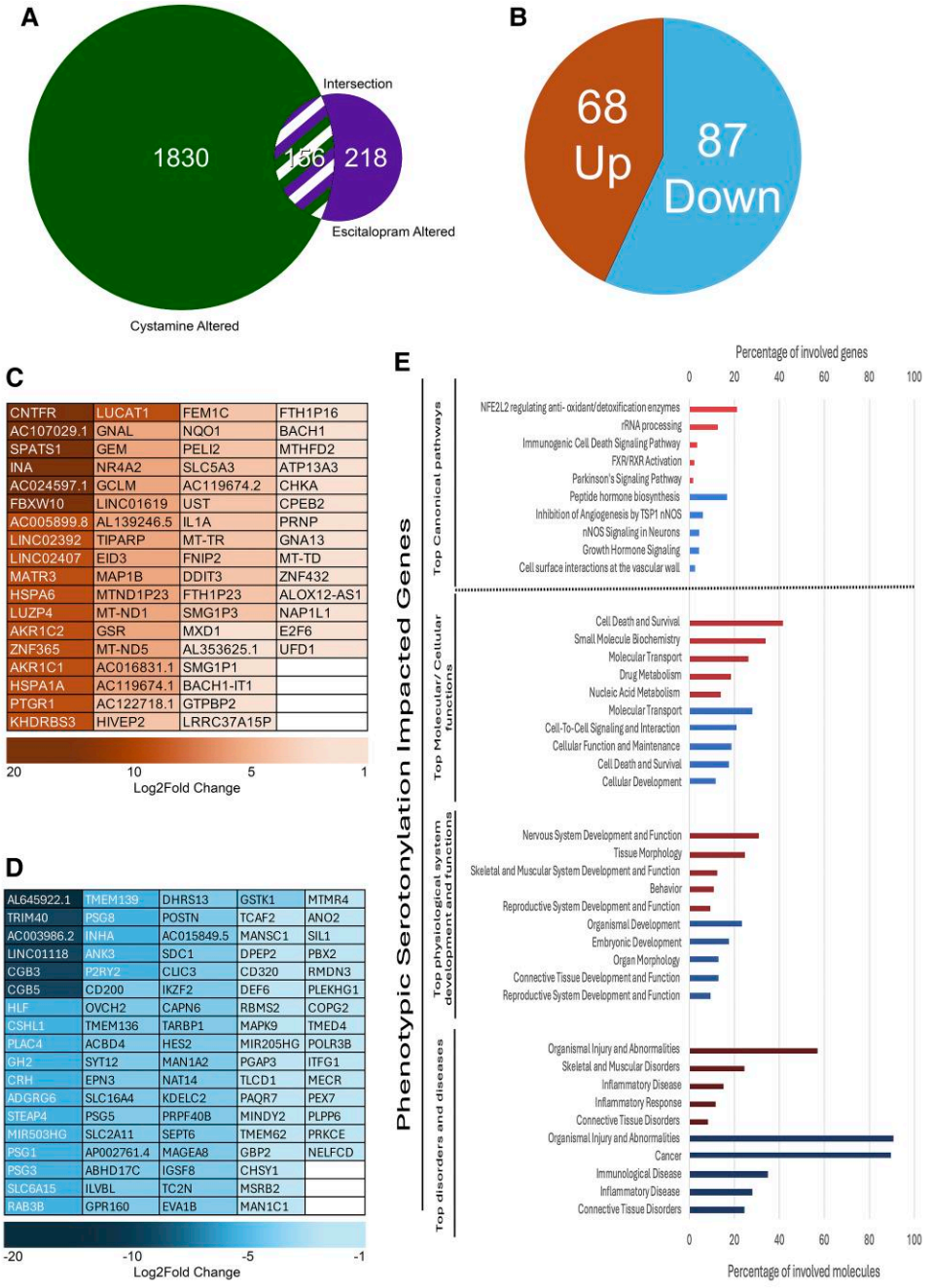

Figure 6. Escitalopram (200 μm) and cystamine (10 mM) altered genes. (A) Venn diagram revealing the 156 overlapping genes altered by both escitalopram and cystamine. (B) Of these 156 common genes, 68 were upregulated and 87 were downregulated by both treatments. (C) Concomitantly upregulated genes. The darker the shading, the greater the fold-change. (D) Concomitantly downregulated genes. The darker the shading, the greater the fold-change. (E) IPA analysis of the 155 concomitantly altered genes.

+3.3 log2 fold change) generates a cellular antioxidant defense. MT-ND1 and MT-ND5 (NADH dehydrogenase subunits 1 and 5; +3.2 and 3.0 log2 fold changes, respectively) are core units of the mitochondrial membrane respiratory chain.

In contrast, many of the genes that were downregulated were involved with cell proliferation, morphogenesis, motility, and growth. Key examples included the following. Protein kinase C epsilon (-1.1 log2 fold change) regulates cell adhesion, motility, migration, and cell cycle. Chondroitin sulfate synthase 1 (-1.4 log2 fold change) is involved with cell proliferation and morphogenesis. MAPK9 (-1.54 log2 fold change) is seen in cell proliferation, differentiation, migration, transformation, and programmed cell death pathways. SEPT6 (Septin 6; -2.1 log2 fold change) is required for cytokinesis. Syndecan 1 (-2.2 log2 fold change) participates with cell proliferation, cell migration, and cell-matrix interactions via its receptor for extracellular matrix proteins. Periostin (-2.3 log2 fold change) induces cell attachment and spreading and plays a role in cell adhesion. Ankyrin 3 (-3.0 log2 fold change) is involved with cell motility, activation, proliferation, contact, and the maintenance of specialized membrane domains. Solute carrier family 6 member 15 (-3.5 log2 fold change) is a sodium-dependent neutral amino acid transporter. GH2 (-4.0 log2 fold change) stimulates

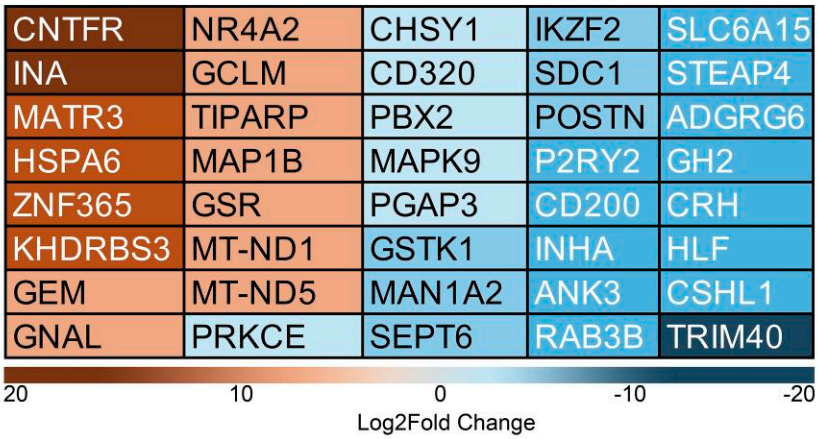

Level	IPA Processes	Genes
Trophoblast	Cellular assembly and organization, cellular function and maintenance, cellular morphology, cell development, cell growth and proliferation	ADGRG6, ANK3, CRH, GEM, GNAL, MAP1B, MAPK9, P2RY2, PRKCE, ZNF365, INA, POSTN, SDC1, RAB3B, GCLM, CD200, INHA, IKZF2, PGAP3, NR4A2, MAN1A2, TIPARP, TRIM40, CD320, GH2, SDC1, HLF, STEAP4, CSHL1, SEPT6
Embryo	Embryonic differentiation, embryonic cell movement, embryonic cell spreading, embryonic invasion, maturation, modification, embryonic cell viability, development	CNTFR, INA, MAP1B, NR4A2, TIPARP, ZNF365, GLCM, GNAL, GEM, GSR, MATR3, CD200, CHSY1, CSHL1, GH2, POSTN, MAN1A2, MAPK9, CRH, PBX2, INHA, P2RY2, GSTK1, IKZF2 PRKCE, SDC1, ANK3
Tissue	Volume, size, morphology, mass, quantity, permeability, diameter, density, density, expansion, healing, area	CNTFR, INA, MAP1B, NR4A2, ZNF365, GCLM, TIPARP, MATR3, GSR, GNAL, GEM
Organ	Development, function, formation, induction, growth, morphogenesis, branching, gonadogenesis, stratification	ANK3, CD200, INHA, MAPK9, P2RY2, POSTN, PRKCE, CRH, CSHL1, GSTK1
Nervous System	Development, differentiation, formation, loss, quantity, firing, morphogenesis, excitation, neuroprotection, neuritogenesis, size, branching, retraction of neurites, maturation/protection of dopaminergic neurons, motor function, extension, length of dendritic spines, stratification of cerebral cortex	ADGRG6, ANK3, CRH, GEM, GNAL, MAP1B, MAPK9, P2RY2, PRKCE, ZNF365, CNTFR, NR4A2, INA, RAB3B, POSTN, SLC6A15, CD200, CD320
Organism	Formation, development, differentiation, volume, size, mass, morphology, conversion, limb development, lean body mass, growth, epithelial-mesenchymal transition, conversion, myelination, extended lifespan, neonatal death, sensorimotor gating, polarization, thickness, elongation, organization neurofilaments, migration neurons, morphology of nervous tissue, electrophysiology of nervous system, long term depression of synapse, mass of brain	ADGRG6, CRH, CSHL1, GH2, IKZF2, INHA, POSTN, PRKCE, RAB3B, CD200, MAPK9, GSTK1, CHSY1, MAN1A2, PBX2, STEAP4, ANK3, P2RY2, PGAP3, SDC1
Behavior	Operant performance, passive avoidance learning, hyperactivity, locomotion, abnormal posture	CNTFR, GNAL, NR4A2
Systemic Diseases	Cancer, epithelial mesenchymal transition, organismal injury and abnormalities, inflammatory response, immunological disease, hematological disease	ANK3, CD200, CD320, CHSY1, GEM, HLF, IKZF2, INA, INHA, MT-ND1, MT-ND5, POSTN, PRKCE, SEPTIN6, STEAP4, ZNF365, CNTFR, GSR, MAP1B, NR4A2, SDC1 SLC6A15, RAB3B, PGAP3, CRH, ADGRG6, PBX2, TRIM40, MAPK9, P2RY2, GSTK1, HSPA6, CSHL1, MAN1A2, TIPARP, GNAL, GH2, PBX2, KHDRBS3, HSPA6
Neurologic Diseases	Parkinson's, Alzheimer's, ALS, psychological disorders (e.g., depression, ASD)	MT-ND1, MT-ND5, NR4A2, MAP1B, MATR3, GNAL, INA, HSPA6, GSR

Figure 7. The final 40 genes concomitantly altered by escitalopram (200 μm) and cystamine (10 mM) treatment. Based on IPA analysis, the 40 genes listed in the top grid appear to be most involved with pathways that can impact trophoblast growth and differentiation. The darker the shading, the greater the fold-change. The lower table represents the nonexhaustive IPA focused processes for these final 40 genes presented in a hierarchical list from the single trophoblast up through the embryo and organism, through behavior, and ending with systemic and neurologic diseases.

body growth by inducing IGF1 secretion. Chorionic somatomammotropin hormone like 1 (−4.51 log2 fold change) is a placenta-specific growth factor.

Overall, IPA (Fig. 7, lower panel) confirmed the most frequent top cellular functions of those genes impacted by serotonylation were related to cell spreading, flattening, morphogenesis, cell morphology, shape, size, cell proliferation, differentiation, development, formation, and growth; that the top developmental functions of those genes were related to embryonic development, embryonic cell differentiation, embryonic cell movement, embryonic cell spreading, embryonic cell invasion, embryonic cell maturation and modification, embryonic cell viability, colony formation, organismal, tissue and organ development; the top systemic disorders of those genes were related to cancer, epithelial-mesenchymal transition, injury, hematological, immunological responses, inflammatory responses; and the top neurologic disorders of these genes were related to neuronal development, function, behaviors, and neurological, psychological and hereditary disorders (including Parkinson disease, Alzheimer disease, amyotrophic lateral sclerosis, and autism spectrum disorder).

Discussion

Employing purified human cytotrophoblasts, we have confirmed some of our previously published findings that utilized explant cultures (14). Specifically, we confirmed that (1) trophoblasts take up 5-HT and concentrate it into the nucleus (Fig. 1A, panels e, g, and h); (2) trophoblasts do not contain immunoreactive TPH-1; and (3) syncytiotrophoblasts express both cytoplasmic MAOA and SERT. Working with purified human cytotrophoblasts allowed us to extend these findings to better understand why 5-HT is concentrated into the trophoblast nucleus and what may be the effects of this localization.

The work of Maze and colleagues (13, 15) suggested an explanation for the concentrating of 5-HT into trophoblast nuclei: serotonylation. And they went on to demonstrate that placental H3 was a major substrate of the serotonylation reaction in the mouse placenta. We therefore started our exploration of serotonylation by investigating the effects of cystamine—which blocks serotonylation—on the nuclear localization of 5-HT in trophoblast explant cultures. While control cultures revealed the expected uptake of 5-HT into both the syncytiotrophoblast and cytotrophoblast cytoplasm, as well as the strong nuclear localization in the cytotrophoblasts (Fig. 2A, panels a and c), the addition of the serotonylation inhibitor cystamine diminished and ultimately eliminated the nuclear staining in these trophoblasts. Immunoprecipitation experiments utilizing purified human cytotrophoblasts suggested that 5-HT was covalently attached to H3 since reciprocal IP experiments with both anti-5-HT and anti-H3 antibodies resulted in similar bands at approximately 17 and 18 kDa (Fig. 2D). This reaction was not specific to H3 as we saw that anti-ferritin precipitated H3, while conversely anti-H3 precipitated ferritin, suggesting that H3 and ferritin also form a complex in these cells. That we could not successfully complete the IP reaction without adding DNase (see Fig. 2C) suggested that serotonylated H3 and ferritin are tightly associated with DNA in the cytotrophoblasts studied. H3 appears to be serotonylated at the glutamine 5 site in cultured trophoblasts as we were able to stain H3 with an anti-H3Q5ser antibody (Fig. 2E). The intensity of the serotonylation of H3 was decreased by inhibiting the serotonylation reaction with cystamine, as well as by decreasing the uptake of 5-HT through blocking the 5-HT transporter (SERT).

As others have shown in other model systems (13, 15), we have demonstrated that the serotonylation pathway alters gene expression in cultured trophoblasts. Of the 38 524 mRNAs produced by cultured trophoblasts in a 2-day period, blocking 5-HT uptake into these cells by inhibiting the serotonin transporter by escitalopram significantly altered the expression of 374 genes. More impressively, blocking serotonylation itself with cystamine significantly altered the expression of 1986 (5.2%) of the total. An informed selection (Fig. 3B) revealed that some genes were very highly expressed (eg, glycoprotein alpha, ferritin light chain, mitochondrial oxidase, aromatase), some were upregulated (eg, heat shock 90alpha 1, ubiquitin B, histone H3), some downregulated (eg, pregnancy specific ß1-glycoprotein 5, syndecan 1, transglutaminase 2), some remained unchanged (eg, ferritin light chain, aromatase, cathepsin B), while others were expressed at very low levels, if at all (eg, TPH1, TPH2).

Utilizing purified human cytotrophoblasts, a strength of this research, afforded us the opportunity to critically evaluate the impact of altering the expression of these genes in one cell type. Organ perfusion and explant culture studies can be misleading since many cell types are present in such experiments. Validation of this statement was seen when we blocked serotonin influx by escitalopram, resulting in the drastic inhibition of the morphologic differentiation of these cells (Fig. 4A). Under normal circumstances, purified human cytotrophoblasts go through a well-documented sequence of morphologic changes, including flattening, aggregating, and syncytialization (21). In the absence of 5-HT uptake this entire process was stopped. This, along with the finding that these cells do not express TPH mRNA (Fig. 3B), strongly challenges the notion that trophoblasts make their own 5-HT via biosynthesis (41). Our finding of a few 5-HT-positive macrophages in our trophoblast cultures (Fig. 4A, panel d and f insets) suggests why previous authors may have thought that the placenta produces 5-HT. The low levels of 5-HT synthesis seen in the mouse placentas in these previous studies (41) may have been the result of resident macrophages, which are known to import tryptophan and convert it to 5-HT (42). It is possible that this also occurs in the human placenta as the chorionic villi are known to contain large numbers of resident macrophages, also called Hofbauer cells (22).

We also provided strong evidence that human cytotrophoblasts take 5-HT up through the same serotonin transporter that is present in all other cells that utilize SERT for 5-HT influx (Fig. 4B and 4C). It was interesting to note that 5-HT influx decreased dramatically over 4 days of culture (Fig. 4D), a time in which cytotrophoblasts are converted almost completely to syncytiotrophoblasts. Over this same period, increasing amounts of SERT could be seen localized to the cytoplasm (Fig. 1B, panels q-t). Because these same cells can transport 5-HT in the intact human placenta (14), one might conclude that SERT exists in a dynamic balance between surface membrane and cytoplasmic fractions, as suggested by previous studies (43). Therefore, the amount of transport active SERT may depend on several factors, including the state of trophoblast differentiation. For example, freshly purified cytotrophoblasts that are the closest representations of in situ cytotrophoblasts express very strong SERT cell surface

staining (Fig. 1A, panel d) suggesting that these cells avidly transport 5-HT. This is consistent with our observation of large amounts of 5-HT within these cells when explants were exposed to exogenous 5-HT (Fig. 2A, panels a and c), reconfirming our earlier observations (14).

Our RNA sequencing studies began to shed light on the key genes that were responsible for these morphologic changes (Fig. 4E). When studied with IPA (31), we noted that among the multiple pathways represented by these genes, there were detoxifying and/or cell protection genes on the one hand, and embryonic, tissue, organ, and organismal development, on the other hand (Fig. 4F).

Addition of cystamine to our cultured cytotrophoblasts allowed us to directly assess the impact of blocking serotonylation on these cells. As with escitalopram, the morphologic impact was dramatic (Fig. 5A). Over a period of 72 hours with exposure to increasing amounts of cystamine these cells failed to flatten, aggregate, and syncytialize (Fig. 5B). Interestingly, cystamine exposure functioned like an Ames test (44), preferentially selecting those trophoblasts that were able to import significant quantities of 5-HT (Fig. 5A, panels f, h, and i). That cystamine altered the expression of significantly more genes (1986) compared to escitalopram (374) suggests that blocking serotonylation itself is more impactful than simply decreasing the influx of 5-HT into these cells. However, this difference might also reflect that escitalopram is a highly selective inhibitor of SERT (45) whereas cystamine is a nonspecific reagent that oxidizes free sulfhydryl groups by a process of thiol-disulfide exchange (46). IPA, like what was seen with escitalopram, revealed pathways involved with both detoxification and cell protection, as well as growth, development, and cell cycle (Fig. 5D).

Examination of the genes that were concomitantly altered by both escitalopram and cystamine treatments yielded a most interesting group of genes impacted by serotonylation (Fig. 6). A limitation of our study was that we did not validate the expression of these genes by quantitative PCR. However, homing in on the key genes suggested by IPA yielded an intriguing group of 40 genes (Fig. 7). Assessing each of these genes individually revealed some clear patterns. In general, the genes that were upregulated were involved with cell survival and protection, whereas those genes that were downregulated were involved with cell proliferation, morphogenesis, motility, and growth. These results, therefore, likely explain what we observed when cultured trophoblasts were exposed to these agents: blocking morphologic differentiation. To flatten out, migrate, aggregate, and eventually syncytialize, these cells would need the functions represented by many of these downregulated genes. These treatments also appeared to be very stressful for these cells as many protective, antioxidant, and repair genes were activated in tandem.

Just as knock out experiments reveal what is necessary for biologic and physiologic function (47), genes that were downregulated by both escitalopram and cystamine presumably would be upregulated when these trophoblasts—and by extension the placenta—are exposed to 5-HT. The converse would be true for the genes that were upregulated. Therefore, these results can offer a road map to the impact of 5-HT on the growing placenta, and potentially to the entire organism (Fig. 7). Since the cytotrophoblast is the growing stem cell of the placenta, it is not surprising that we have shown that these cells avidly take up 5-HT and that the genes that are likely to be upregulated by the combination of 5-HT influx, followed by the serotonylation of at least H3, are involved with cell proliferation, morphogenesis, motility, and growth. These processes are critical during pregnancy's initial phases of implantation and placentation (48-50). This then gives a molecular explanation for why we observed so much 5-HT concentrated in the first trimester placental cytotrophoblasts (14): this is the time of critical growth of the placenta. In fact, the placenta remains larger than its passenger fetus up to around 18 to 20 weeks of gestation (51). Put simply, one needs to make the boat before you allow the passenger to board.

This observation may also partly explain why patients who take selective serotonin reuptake inhibitors during pregnancy (such as escitalopram [brand name Lexapro]) have smaller babies than control patients (52). The influx of 5-HT into the placenta appears to play an important role in placental growth, but that is only a waystation on the journey to the embryo and fetus. After 20 weeks of gestation, fetal growth significantly outpaces placenta growth to the point that at term (40 weeks of gestation), the fetus is approximately 6 times heavier than its supporting placenta (53). The presumption, therefore, would be that the continued transport of 5-HT into and through the placenta—and then into the fetal circulation—is an important stimulus for fetal growth. If true, blocking this influx would lead to decreased fetal growth.

Conversely, this observation may also help to explain why placentas from children with autism (54), or at risk for autism (55), might have an increased number of trophoblast inclusions. Trophoblast inclusions are the result of increased numbers of cytotrophoblasts compared to the overlying syncytium, which, by mechanical folding, leads to the formation of an invagination of the trophoblast bilayer (56, 57). When these invaginations are cross-sectioned, trophoblast inclusions are created (58, 59). An increase in 5-HT uptake, along with increased serotonylation of nuclear proteins (including H3), may be the reason for the increased cytotrophoblast proliferation and resultant trophoblast inclusion formation seen in the placentas of children with or at risk for autism (54, 55). It is also plausible that the increased flux of 5-HT into and through the placenta on its way to the embryo or fetus might explain the increased growth of such children, as well as the increased brain folding that has been described in children with autism (60, 61), and possibly other neurologic conditions. Moreover, IPA of our final 40 genes highlighted their involvement in brain development, behavior, and neurological disorders such as autism spectrum disorder, which aligns well with the work of Maze and colleagues on serotonylation of H3, brain development, and depression (13).

If true, these findings might suggest conditions that could promote the development of autism. For example, increased levels of bioavailable 5-HT at the placental surface during pregnancy or lower levels of syncytial trophoblast MAOA (the primary enzyme that degrades 5-HT in the placenta) would result in a higher flux of 5-HT into the embryo and fetus, which in turn could lead to an increase in overall embryonic and fetal growth, and/or an increase in brain growth (2-8).

Although we only examined the human trophoblast in these studies, that many of the genes modulated in this cell by our treatments are also found in pathways observed in many higher organizational levels, including tissues, organs, and the organism—as well as seen in systemic and neurologic diseases—suggests that serotonylation may be a fundamental regulatory pathway that deserves more attention.

Finally, these studies appear to answer the question of why 5-HT is concentrated into the cytotrophoblast nucleus: serotonylation. However, many questions remain, including: (1) besides H3, what other nuclear proteins are serotonylated and what are the consequences of this serotonylation; (2) what regulates the disposition of SERT into the syncytiotrophoblast surface membrane; and (3) what is the nature, function, and consequences of the serotonylated H3-DNA complex?

Acknowledgments

The authors thank the Human Research Protection Program and institutional review board at Yale University for reviewing and approving the ethics and human subject issues for our study. The authors also thank Lauren Perley, Svenja Bockelmann, Jane O'Bryan, Samantha Girasulo, Aliaksandr Kishchanka, MD, Joanne Sheu, MD, MPH, and Molly McAdow, MD, PhD, of the Yale University Reproductive Sciences Biobank for their efficient and constant help in consenting patients at the Yale New Haven Hospital that allowed us to collect fresh, healthy control placentas for these studies. The authors thank the many scientists (especially Antariksh Tyagi who patiently addressed all our concerns and questions during these studies) and staff members of the Yale Center for Genomic Analysis, which is supported by the National Institute of General Medical Sciences of the National Institutes of Health under Award Number 1S10OD030363-01A1. And finally, the authors thank Theodore L. Steck of the University of Chicago for his thoughtful comments on the research and insightful suggestions regarding the manuscript.

Funding

This work was supported by the Fulbright-Monahan Foundation (N.S.M.), the Université de Paris Cité (N.S.M.), and the Reproductive and Placental Research Unit, Yale University School of Medicine (H.J.K.).

Disclosures

No conflicts of interest are reported for any of the authors.

Data Availability

Our RNA sequencing data are freely available in the Dryad Digital Repository: https://doi.org/10.5061/dryad.b8gtht7qb. More detailed raw sequencing data, including the fastq files, are available at the National Institutes of Health National Center for Biotechnology Information Gene Expression Omnibus (NCBI-GEO), accession number GSE299974 (https://www.ncbi.nlm.nih.gov/geo/query/acc.cgi?acc=GSE299974).

References

1. Gauster M, Moser G, Wernitznig S, Kupper N, Huppertz B. Early human trophoblast development: from morphology to function. *Cell Mol Life Sci*. 2022;79(6):345.
2. Yavarone MS, Shuey DL, Sadler TW, Lauder JM. Serotonin uptake in the ectoplacental cone and placenta of the mouse. *Placenta*. 1993;14(2):149-161.
3. Gaspar P, Cases O, Maroteaux L. The developmental role of serotonin: news from mouse molecular genetics. *Nat Rev Neurosci*. 2003;4(12):1002-1012.
4. Cote F, Fligny C, Bayard E, *et al*. Maternal serotonin is crucial for murine embryonic development. *Proc Natl Acad Sci U S A*. 2007;104(1):329-334.
5. Buznikov GA, Lambert HW, Lauder JM. Serotonin and serotonin-like substances as regulators of early embryogenesis and morphogenesis. *Cell Tissue Res*. 2001;305(2):177-186.
6. Lauder JM, Tamir H, Sadler TW. Serotonin and morphogenesis. I. Sites of serotonin uptake and -binding protein immunoreactivity in the midgestation mouse embryo. *Development*. 1988;102(4):709-720.
7. Pfeiffer S, Boyle J, Daly S, Dowd E, Haase J, McLaughlin D. Human amniocytes regulate serotonin levels by active uptake and express genes suggestive of a wider role in facilitating neurotransmitter regulation in the fetal environment. *Stem Cells Dev*. 2011;20(2):341-349.
8. Ori M, De Lucchini S, Marras G, Nardi I. Unraveling new roles for serotonin receptor 2B in development: key findings from Xenopus. *Int J Dev Biol*. 2013;57(9-10):707-714.
9. Liu Y, Wei L, Laskin DL, Fanburg BL. Role of protein transamidation in serotonin-induced proliferation and migration of pulmonary artery smooth muscle cells. *Am J Respir Cell Mol Biol*. 2011;44(4):548-555.
10. Penumatsa K, Abualkhair S, Wei L, *et al*. Tissue transglutaminase promotes serotonin-induced AKT signaling and mitogenesis in pulmonary vascular smooth muscle cells. *Cell Signal*. 2014;26(12):2818-2825.
11. Bader M. Inhibition of serotonin synthesis: a novel therapeutic paradigm. *Pharmacol Ther*. 2020;205:107423.
12. Patra SK. Emerging histone glutamine modifications mediated gene expression in cell differentiation and the VTA reward pathway. *Gene*. 2021;768:145323.
13. Chan JC, Alenina N, Cunningham AM, *et al*. Serotonin transporter-dependent histone serotonylation in placenta contributes to the neurodevelopmental transcriptome. *J Mol Biol*. 2024;436(7):168454.
14. Kliman HJ, Quaratella SB, Setaro AC, *et al*. Pathway of maternal serotonin to the human embryo and Fetus. *Endocrinology*. 2018;159(4):1609-1629.
15. Farrelly LA, Thompson RE, Zhao S, *et al*. Histone serotonylation is a permissive modification that enhances TFIID binding to H3K4me3. *Nature*. 2019;567(7749):535-539.
16. Walther DJ, Peter JU, Winter S, *et al*. Serotonylation of small GTPases is a signal transduction pathway that triggers platelet alpha-granule release. *Cell*. 2003;115(7):851-862.
17. Paulmann N, Grohmann M, Voigt JP, *et al*. Intracellular serotonin modulates insulin secretion from pancreatic beta-cells by protein serotonylation. *PLoS Biol*. 2009;7(10):e1000229.
18. Kim DA, McClure WG III, Neighoff JB, Vaidya D, Williams MS. Platelet response to serotonin in patients with stable coronary heart disease.*Am J Cardiol*. 2014;114(2):181-186.
19. Widmann R, Sperk G. Cysteamine-induced decrease of somatostatin in rat brain synaptosomes *in vitro*. *Endocrinology*. 1987;121(4):1383-1389.
20. Kliman HJ, Sammar M, Grimpel YI, *et al*. Placental protein 13 and decidual zones of necrosis: an immunologic diversion that may be linked to preeclampsia. *Reprod Sci*. 2012;19(1):16-30.
21. Kliman HJ, Nestler JE, Sermasi E, Sanger JM, Strauss JF, 3rd. Purification, characterization, and *in vitro* differentiation of cytotrophoblasts from human term placentae. *Endocrinology*. 1986;118(4):1567-1582.
22. Tang Z, Tadesse S, Norwitz E, Mor G, Abrahams VM, Guller S. Isolation of hofbauer cells from human term placentas with high yield and purity. *Am J Reprod Immunol*. 2011;66(4):336-348.
23. Yuan I, Horng CT, Chen VC, *et al*. Escitalopram oxalate inhibits proliferation and migration and induces apoptosis in non-small cell lung cancer cells. *Oncol Lett*. 2018;15(3):3376-3382.

24. Zhang YW, Rudnick G. Serotonin transporter mutations associated with obsessive-compulsive disorder and phosphorylation alter binding affinity for inhibitors. *Neuropharmacology*. 2005;49(6):791-797.
25. Kim D, Paggi JM, Park C, Bennett C, Salzberg SL. Graph-based genome alignment and genotyping with HISAT2 and HISAT-genotype. *Nat Biotechnol*. 2019;37(8):907-915.
26. Pertea M, Pertea GM, Antonescu CM, Chang TC, Mendell JT, Salzberg SL. StringTie enables improved reconstruction of a transcriptome from RNA-seq reads. *Nat Biotechnol*. 2015;33(3):290-295.
27. Frankish A, Diekhans M, Ferreira AM, *et al*. GENCODE reference annotation for the human and mouse genomes. *Nucleic Acids Res*. 2019;47(D1):D766-D773.
28. Love MI, Huber W, Anders S. Moderated estimation of fold change and dispersion for RNA-seq data with DESeq2. *Genome Biol*. 2014;15(12):550.
29. Zhao Y, Li MC, Konate MM, *et al*. TPM, FPKM, or normalized counts? A comparative study of quantification measures for the analysis of RNA-seq data from the NCI patient-derived models repository. *J Transl Med*. 2021;19(1):269.
30. Hochberg Y, Benjamini Y. More powerful procedures for multiple significance testing. *Stat Med*. 1990;9(7):811-818.
31. Krämer A, Green J, Pollard J Jr, Tugendreich S. Causal analysis approaches in ingenuity pathway analysis. *Bioinformatics*. 2014;30(4):523-530.
32. Folk JE. Transglutaminases. *Annu Rev Biochem*. 1980;49(1):517-531.
33. Sakbun V, Ali SM, Lee YA, Jara CS, Bryant-Greenwood GD. Immunocytochemical localization and messenger ribonucleic acid concentrations for human placental lactogen in amnion, chorion, decidua, and placenta. *Am J Obstet Gynecol*. 1990;162(5):1310-1317.
34. Watts SW, Priestley JR, Thompson JM. Serotonylation of vascular proteins important to contraction. *PLoS One*. 2009;4(5):e5682.
35. Fibach E, Konijn AM, Rachmilewitz EA. Changes in cellular ferritin content during myeloid differentiation of human leukemic cell lines. *Am J Hematol*. 1985;18(2):143-151.
36. Surguladze N, Thompson KM, Beard JL, Connor JR, Fried MG. Interactions and reactions of ferritin with DNA. *J Biol Chem*. 2004;279(15):14694-14702.
37. Gu H, Wall SC, Rudnick G. Stable expression of biogenic amine transporters reveals differences in inhibitor sensitivity, kinetics, and ion dependence. *J Biol Chem*. 1994;269(10):7124-7130.
38. Muma NA, Mi Z. Serotonylation and transamidation of other monoamines. *ACS Chem Neurosci*. 2015;6(7):961-969.
39. Jeitner TM, Pinto JT, Cooper AJL. Cystamine and cysteamine as inhibitors of transglutaminase activity *in vivo*. *Biosci Rep*. 2018;38(5):BSR20180691.
40. Wang HM, Liu WZ, Tang FT, Sui HJ, Zhan XJ, Wang HX. Cystamine slows but not inverses the progression of monocrotaline-induced pulmonary arterial hypertension in rats. *Can J Physiol Pharmacol*. 2018;96(8):783-789.
41. Bonnin A, Goeden N, Chen K, *et al*. A transient placental source of serotonin for the fetal forebrain. *Nature*. 2011;472(7343):347-350.
42. Martins E Jr, Ferreira AC, Skorupa AL, Afeche SC, Cipolla-Neto J, Costa Rosa LF. Tryptophan consumption and indoleamines production by peritoneal cavity macrophages. *J Leukoc Biol*. 2004;75(6):1116-1121.
43. Anderluh A, Klotzsch E, Ries J, *et al*. Tracking single serotonin transporter molecules at the endoplasmic reticulum and plasma membrane. *Biophys J*. 2014;106(9):L33-L35.
44. Ames BN, Lee FD, Durston WE. An improved bacterial test system for the detection and classification of mutagens and carcinogens. *Proc Natl Acad Sci U S A*. 1973;70(3):782-786.
45. Hyttel J, Bogeso KP, Perregaard J, Sanchez C. The pharmacological effect of citalopram residues in the (S)-(+)-enantiomer. *J Neural Transm Gen Sect*. 1992;88(2):157-160.
46. Sharma R, Kodavanti UP, Smith LL, Mehendale HM. The uptake and metabolism of cystamine and taurine by isolated perfused rat and rabbit lungs. *Int J Biochem Cell Biol*. 1995;27(7):655-664.
47. Hall B, Limaye A, Kulkarni AB. Overview: generation of gene knockout mice. *Curr Protoc Cell Biol*. 2009;44(1):19.12.1-19.12.17.
48. Bischof P, Campana A. A model for implantation of the human blastocyst and early placentation. *Hum Reprod Update*. 1996;2(3):262-270.
49. Chen ST, Ran F, Shi WW, *et al*. Tryptophan in the mouse diet is essential for embryo implantation and decidualization. *Front Endocrinol (Lausanne)*. 2024;15:1356914.
50. Basu B, Desai R, Balaji J, *et al*. Serotonin in pre-implantation mouse embryos is localized to the mitochondria and can modulate mitochondrial potential. *Reproduction*. 2008;135(5):657-669.
51. Boyd JD, Hamilton WJ. *The Human Placenta*. W. Heffer & Sons Ltd; 1970.
52. Boukhris T, Sheehy O, Mottron L, Bérard A. Antidepressant use during pregnancy and the risk of autism spectrum disorder in children. *JAMA Pediatr*. 2016;170(2):117-124.
53. Hutcheon JA, McNamara H, Platt RW, Benjamin A, Kramer MS. Placental weight for gestational age and adverse perinatal outcomes. *Obstet Gynecol*. 2012;119(6):1251-1258.
54. Anderson GM, Jacobs-Stannard A, Chawarska K, Volkmar FR, Kliman HJ. Placental trophoblast inclusions in autism spectrum disorder. *Biol Psychiatry*. 2007;61(4):487-491.
55. Walker CK, Anderson KW, Milano KM, *et al*. Trophoblast inclusions are significantly increased in the placentas of children in families at risk for autism. *Biol Psychiatry*. 2013;74(3):204-211.
56. Kliman HJ, Segel L. The placenta may predict the baby. *J Theor Biol*. 2003;225(1):143-145.
57. Rejniak KA, Kliman HJ, Fauci LJ. A computational model of the mechanics of growth of the villous trophoblast bilayer. *Bull Math Biol*. 2004;66(2):199-232.
58. Kliman HJ, Firestein MR, Hofmann KM, *et al*. Trophoblast inclusions in the human placenta: identification, characterization, quantification, and interrelations of subtypes. *Placenta*. 2021;103:172-176.
59. Firestein MR, Kliman HJ, Sania A, *et al*. Trophoblast inclusions and adverse birth outcomes. *PLoS One*. 2022;17(3):e0264733.
60. Awate SP, Win L, Yushkevich P, Schultz RT, Gee JC. 3D cerebral cortical morphometry in autism: increased folding in children and adolescents in frontal, parietal, and temporal lobes. *Med Image Comput Comput Assist Interv*. 2008;11(Pt 1):559-567.
61. Nordahl CW, Dierker D, Mostafavi I, *et al*. Cortical folding abnormalities in autism revealed by surface-based morphometry. *J Neurosci*. 2007;27(43):11725-11735.